Avert the Dirt

Maan, Anna M. C.

DOI:
10.33612/diss.708771517


3

Chapter 3

Polymer Synthesis and Modification

In order to fabricate and optimize the polymer-based antifouling coatings introduced in this thesis, a library of homopolymers and diblock copolymers with distinct block ratios and lengths needs to be synthesized. This library includes PS, PMMA, PAA, PS-*b*-PAA, PMMA-*b*-PAA, PDMAEMA-*b*-PEG, PDMAEMA-*b*-POEGMA, and PDMAEMA-*b*-PMPC. Here, we discuss suitable polymerization techniques and protocols to synthesize these polymers in high purity and with narrow distributions. Additionally, we briefly touch upon two specific polymer modifications, namely quaternization and CTA end-group removal.

3.1. Introduction

Due to the significant environmental and economic impact of fouling (i.e., undesired adhesion), many new strategies have been developed to reduce or even inhibit these contaminating and destructive processes.[1,2] Polymers present promising candidates to achieve this aim. These macromolecules, consisting of a large number of small chemical units (monomers) linked together, are affordable, nontoxic, biocompatible, easy to process, have a wide-range efficacy, and their functionalities are easily modified to suit the application of interest.[3–5] Specifically when densely end-grafted to an interface, either chemically or physically, the obtained polymer brush can provide both a steric and energetic barrier to prevent fouling agents from adsorbing.[6–14]

However, the strength of the repulsive forces that the polymer brush exerts on approaching fouling particles is determined by two key parameters: the brush thickness (i.e., brush height) and the grafting density.[15–17] To illustrate this, while high-density and thick brushes are impenetrable, sparse and low-density brushes would still permit the diffusion of particles through the brush, causing adsorption to the underlying surface.[8,9] Thus, to obtain highly effective antifouling brushes, the grafting density should be maximized. Unfortunately, in the case of physisorbed systems, a trade-off exists between the grafting density and stability: a short anchoring block could produce a sufficiently dense brush, but the low adsorption energy between the polymer and surface may cause desorption over time, resulting in the loss of its antifouling property. On the other hand, when extending the anchoring block in order to increase the binding energy, the polymer will crowd the interface, thereby preventing the formation of a dense brush.[16,18–21]

Hence, to manage the delicate balance between the adhesion strength and grafting density of the adsorbing polymers, strict control over the block lengths (i.e., molecular weight) and dispersity of the synthesized polymers is essential. Reversible deactivation radical polymerization (RDRP), also known as controlled radical polymerization (CRP), offers such a high degree of control. This type of polymerization combines the benefits of living polymerizations (i.e., suppressing termination) with the versatility and convenience of a radical process.[22–25] It enables the synthesis of polymers with well-defined chain lengths, distributions, compositions, architectures, and end-group fidelity. Moreover, the reactions can proceed under relatively mild conditions and are compatible with an extensive range of monomers in varying solvents.[22–29]

This chapter will mainly focus on the experimental procedures and analysis of an extensive collection of polymers used in this thesis. First, two well-known CRP methods, i.e., RAFT and ATRP, are introduced and the choice of specific RAFT agents is explained. This is followed by a description of the RAFT synthesis of homopolymers (PS, PMMA, PAA, and PDMAEMA) and diblock copolymers (PS-*b*-PAA, PMMA-*b*-PAA, PDMAEMA-*b*-POEGMA, and PDMAEMA-*b*-PMPC), the ATRP synthesis of PDMAEMA-*b*-PEG, the quaternization of weak polyelectrolytes to give strong polyelectrolytes, and finally the end-group removal of RAFT agents via a photocatalytic strategy. For reference, an overview of the complete polymer library is provided in Appendix A (Table A1).

3.2. Theory – Controlled Radical Polymerization

3.2.1. RAFT and ATRP: Two Common CRP Techniques

The two most common CRP techniques are reversible addition-fragmentation chain transfer (RAFT) polymerization and atom transfer radical polymerization (ATRP). A simplified schematic representation of these methods is depicted in Figure 3.1. Both techniques ensure continuous growth and uniformity of polymer chains in a similar way, namely via a dynamic equilibrium between active and dormant chains, and yet the mechanism used to control chain growth is quite distinct (Figure A1).[22,26,28] In the case of RAFT, control over chain growth is achieved via a degenerate chain transfer mechanism, which involves a fast exchange between growing radical chains (P_n• and P_m•) via the RAFT agent. The RAFT agent, or chain transfer agent (CTA), determines the success of this polymerization, and its efficacy is strongly correlated to the selection of the radical leaving "R-group" and the activating and stabilizing "Z-group" contained within this thiocarbonylthio moiety.[22–27] In contrast, ATRP is a catalytic process that involves an equilibrium between an ATRP initiator (R-X) and radicals that are produced by the cleavage of the R-X bond catalyzed by a transition metal complex ($LCu^{I}X$, the activator).[26,28–30] For a more elaborate discussion on each technique, we refer to some excellent reviews that have been published previously.[22,26,31–33]

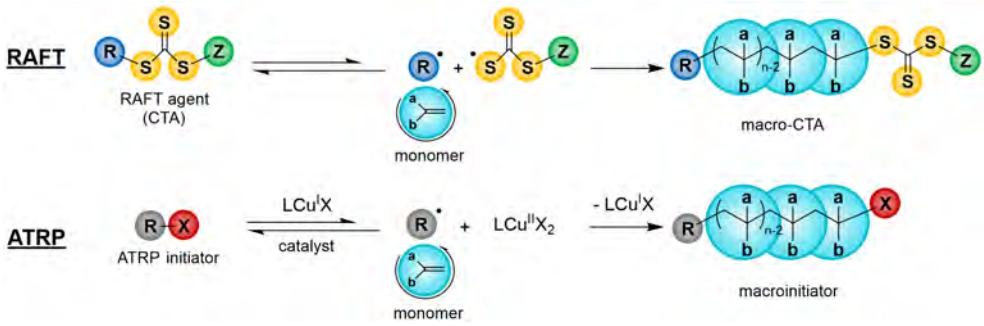

Figure 3.1. Simplified schematic representation of the RAFT and ATRP techniques. The trithiocarbonate RAFT agent is composed of a radical leaving group (R) and stabilizing group (Z), while ATRP involves a transition metal catalyst, a complexing ligand (L), and a halogen counterion (X).

3.2.2. Choice of RAFT Agents

Since RAFT polymerization works exceptionally well for styrene and (meth)acrylate monomers, it was decided to use this technique for the preparation of polystyrene (PS), poly(acrylic acid) (PAA), poly(methyl methacrylate) (PMMA), poly(2-(dimethylamino)ethyl methacrylate) (PDMAEMA), polystyrene-*block*-poly(acrylic acid) (PS-*b*-PAA), poly(methyl methacrylate)-*block*-poly(acrylic acid) (PMMA-*b*-PAA), poly(2-(dimethylamino)ethyl methacrylate)-*block*-poly(oligo(ethylene glycol) methyl ether methacrylate) (PDMAEMA-*b*-POEGMA), and poly(2-(dimethylamino)ethyl

methacrylate)-*block*-poly(2-methacryloyloxyethyl phosphorylcholine) (PDMAEMA-*b*-PMPC).[24–26] Two types of trithiocarbonate RAFT agents were employed within these syntheses: commercially available 2-(dodecylthiocarbonothioylthio)-2-methylpropionic acid (DDMAT) containing a relatively large dodecyl chain, and the on-site synthesized 2-cyanopropan-2-yl propyl trithiocarbonate (CPP-TTC) that contains a smaller propyl tail. DDMAT was mainly used in the synthesis of PS and PS-*b*-PAA, since it is an effective, readily available, and affordable RAFT agent for polymerizing styrene. However, since RAFT polymers are always end-capped with the Z-group of the CTA, which in the case of DDMAT involves a C12 chain, removal of these chain-end functionalities may be necessary: the incorporated end-groups may affect the solubility and self-assembly behavior of the RAFT polymer (e.g., critical aggregation concentration and micellar shape). Especially for low molecular weight diblock copolymers, the presence of a hydrophobic end-group could force the polymer to self-assemble into flower-like micelles (ABA triblock character) rather than the anticipated spherical micelles (AB diblock character).[22–24,34,35] To be able to investigate the possible influence of incorporated DDMAT end-groups on the self-assembly and adsorption behavior of PS-*b*-PAA micelles as well as the antifouling efficacy of the formed coating (Chapter 5), the trithiocarbonate end-group was removed according to a previously reported metal-free photocatalytic strategy (Figure 3.2). In the presence of visible light, the elegant interplay between the amine, tertiary phosphine, and photocatalyst (Eosin Y) enables the successful desulfurization of the polymer.[36]

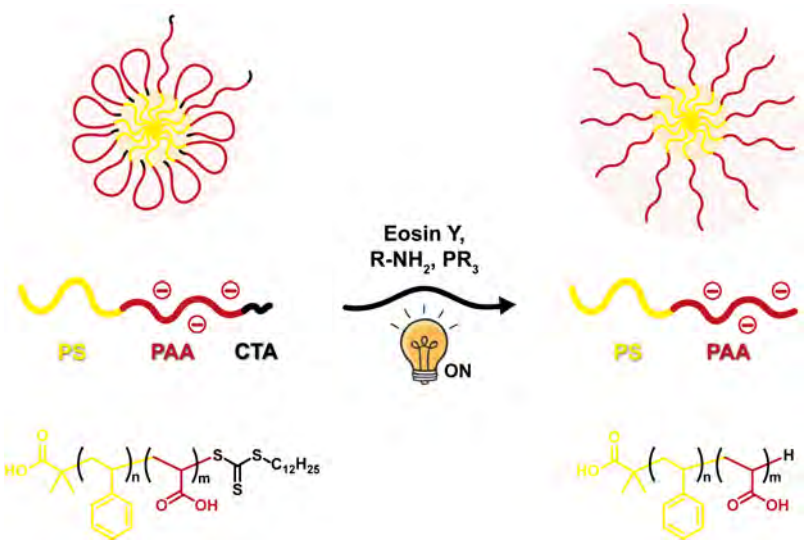

Figure 3.2. Schematic representation of the RAFT end-group removal from PS-*b*-PAA diblock copolymers via a photocatalytic strategy.

The CPP-TTC RAFT agent was specifically selected to synthesize the methacrylate polymers (PMMA, PMMA-*b*-PAA, PDMAEMA, PMDAEMA-*b*-POEGMA, and PDMAEMA-*b*-PMPC), since its R-group presents a better leaving group than the one connected to

DDMAT, which will facilitate a faster initiation and therefore improves the dispersity of the resulting polymers. In addition, it was used to minimize any possible side effect originating from the incorporated RAFT agent (C3 versus C12 chain). Regarding the PEG-*b*-PDMAEMA diblock copolymers, however, it was decided to synthesize these copolymers via ATRP, since an efficient one-step route for the conversion of commercially available PEG-OH into PEG-Br macroinitiator was readily available.[37] Figure 3.3 provides an overview of all used monomers and reagents.

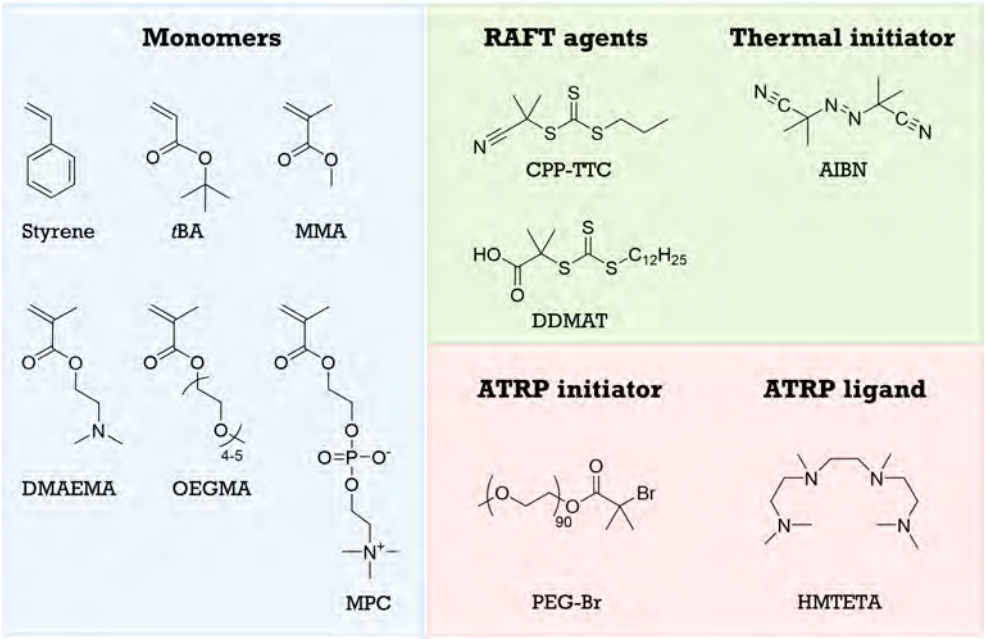

Figure 3.3. Overview of the structural formulas of all monomers and reagents used in the syntheses, including the selected RAFT agents (CTAs), thermal initiator, ATRP initiator, and ATRP ligand.

3.3. Experimental Section

3.3.1. Materials

Azobisisobutyronitrile (AIBN, 98%), aluminum oxide (Al_2O_3, basic, activated), 2-(dodecylthiocarbonothioylthio)-2-methylpropionic acid (DDMAT, 98%), 1,4-dioxane (≥99.0%), 2-(dimethylamino)ethyl methacrylate (DMAEMA, hydroquinone stabilized, 98%), 1,1,4,7,10,10-hexamethyltriethylenetetramine (HMTETA, 97.0%), *N,N*-dimethylformamide (DMF, ≥99.9%), copper(I) bromide (CuBr, 98%), 1-propanethiol (99.0%), sodium hydroxide (NaOH, pellets, ≥98%), carbon disulfide (CS_2, ≥99.9%), iodine flakes (≥99%), sodium thiosulfate ($Na_2S_2O_3$, ≥98.0%), magnesium sulfate ($MgSO_4$, ≥99.5%), iodomethane (MeI, ≥99%), deuterated chloroform ($CDCl_3$, 99.8% D), deuterated dimethyl sulfoxide (DMSO-d_6, 99.5% D), deuterium chloride (DCl, 35 wt% in D_2O, ≥99%), deuterium oxide (D_2O, 99.9%), oligo(ethylene glycol) methyl ether methacrylate (OEGMA, M_n = 300 g mol^{-1}), 2-methacryloyloxyethyl phosphorylcholine (MPC, 97%), methanol-d_4 (≥99.8%), α-bromoisobutyryl bromide (B*i*BB, 98%), triethylamine (TEA, ≥99.5%), Eosin Y (photocatalyst, 99%), hexylamine (99%), and tri-*n*-butylphosphine (93.5%) were purchased from Sigma-Aldrich. Styrene (4-*tert*-butylcatechol stabilized, 99.0%) and methyl methacrylate (MMA, stabilized, 99%) were purchased from Acros Organics. Methanol (≥99.9%), *n*-pentane (99%), isopropanol (*i*-PrOH, ≥99.8%), *n*-hexane (99%), diethyl ether (Et_2O, HPLC grade), ethyl acetate (EtOAc, HPLC grade), acetone (HPLC grade), and dichloromethane (DCM, HPLC grade) were purchased from Macron Fine Chemicals. Anisole (≥99%) was sourced from Merck. Absolute ethanol (99.9%) was purchased from J.T. Baker. Tetrahydrofuran (THF, BHT stabilized, ≥99.8%) and 1,1,1,3,3,3-hexafluoro-2-propanol (HFIP, ≥99.8%) were purchased from Biosolve. Aliquat® 336 was obtained from Alfa Aesar. Poly(ethylene glycol) monomethylether (PEG_{90}, M_n = 4.01 kg mol^{-1}, $Đ$ = 1.05) and *tert*-butyl acrylate (*t*BA, MEHQ stabilized, 98%) were purchased from TCI. Hydrochloric acid solution (HCl, 37%) was sourced from Boom. Dry DCM was obtained through a MB-SPS 800 purification machine from MBraun, equipped with HPLC grade DCM from Ossum Chemicals. The dialysis tubing (Spectra/Por 6, MWCO = 1 kDa) was purchased from Spectrum Chemicals.

AIBN was recrystallized twice from methanol. All commercially available monomers were passed over a short basic aluminum oxide column to remove the inhibitor directly before their use in the polymerizations, except for MPC. All other chemicals were used as received.

3.3.2. Characterization

Proton and Carbon-13 Nuclear Magnetic Resonance (^{1}H NMR and ^{13}C NMR) Spectroscopy. NMR spectra were recorded on an Agilent 400-MR 400 MHz spectrometer operating at room temperature (298 K). Polymer samples were dissolved in the appropriate deuterated solvent with a concentration of roughly 20 mg mL^{-1}. The resulting spectra were analyzed using MestreNova software (version 14.2.0).

Gel Permeation Chromatography (GPC). To determine the relative molecular weight and the molecular weight distribution (i.e., dispersity; *Đ*) of the synthesized polymers, GPC was performed in DMF (containing 0.01 M LiBr) on a Viscotek GPCMax system equipped with model 302 TDA detectors and two columns (PolarGel L and M, 8 µm 30 cm) from Agilent Technologies at a flow rate of 1 mL min^{-1}. The columns and detectors were maintained at a temperature of 50 °C. Near monodisperse poly(methyl methacrylate) standards from Polymer Standards Service were used for the construction of a calibration curve based on conventional calibration. All polymer samples were dissolved in DMF-LiBr ($c \approx 2–3$ mg mL^{-1}) at least one day in advance and were passed through a 0.20 µm PTFE filter prior to injection. Data acquisition and calculations were performed using Viscotek Omnisec software (version 5.0).

Attenuated Total Reflection–Fourier Transform Infrared (ATR-FTIR) Spectroscopy. ATR-FTIR spectra were recorded on a Bruker VERTEX 70 spectrometer, equipped with an ATR diamond single reflection module. The spectra were collected in the range of 4000–400 cm^{-1} with a spectral resolution of 2 cm^{-1} and using 64 scans for each sample. Atmospheric compensation and baseline corrections (concave rubberband correction, 10 iterations) were applied to the collected spectra using Bruker's OPUS spectroscopy software (version 7.5).

UV-Vis Spectroscopy. UV-Vis spectra were recorded at room temperature on an Analytik Jena Specord 210 Plus spectrophotometer using 10 x 10 mm quartz cuvettes. Polymer solutions were prepared in THF at appropriate concentrations in order to keep the absorbance below one. Prior to the measurement, a proper baseline was established by measuring the reference solution (i.e., solvent), after which the absorption spectra of the polymer solutions were recorded between 200 and 500 nm, with 1 nm intervals and a speed of 10 nm s^{-1}. The integration time was set to 0.1 s, with a slit of 1 nm. Obtained spectra were subsequently analyzed using Aspect UV software (version 1.4.4.8572).

Dynamic Light Scattering (DLS). DLS measurements were performed on a Malvern Panalytical Zetasizer Ultra, equipped with a helium-neon laser (λ = 633 nm) and an avalanche photodiode detector. Unfiltered polymer solutions with concentrations of 10 mg mL^{-1} in ethanol were transferred to 10 x 10 mm quartz cuvettes. The samples were recorded fivefold in the noninvasive backscattering (NIBS) mode at 25 °C after a 120 s equilibration time. Results were analyzed using ZS Xplorer software (version 3.1).

3.4. RAFT – Synthesis and Analysis

3.4.1. Synthesis of the CPP-TTC Chain Transfer Agent

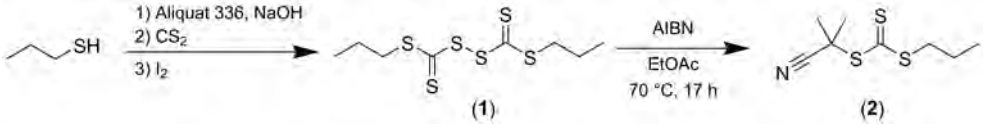

Scheme 3.1. Reaction scheme for the synthesis of the CPP-TTC chain transfer agent.

The 2-cyanopropan-2-yl propyl trithiocarbonate (CPP-TTC, M_w = 219.4 g mol^{-1}) RAFT agent was synthesized according to a previously reported two-step procedure with some minor changes added.[38]

The first step involved the synthesis of an intermediate product, bis(propylsulfanylthiocarbonyl) disulfide (**1**). Under nitrogen atmosphere and at room temperature, 1-propanethiol (1 eq., 39.6 mmol, 3.02 g) and 30 mL diethyl ether were charged in a 250 mL three-neck round-bottom flask, equipped with a stirring bar, two stoppers, and a tap connected to nitrogen. Three drops of Aliquat 336 (phase-transfer catalyst) were added to the flask, followed by the dropwise addition of a 25 wt% hydroxide solution (1 eq., 40.2 mmol, 6.38 g). The resulting slightly pink two-layer system was subsequently stirred for 30 min. Carbon disulfide (1.1 eq., 43.7 mmol, 3.33 g) was dissolved in 10 mL of diethyl ether and slowly added to the stirred mixture over the course of 30 min. The aqueous layer turned bright yellow instantaneously, and gradually turned orange while addition continued. The reaction mixture was diluted with 10 mL of diethyl ether. Afterwards, iodine flakes (0.56 eq., 22.3 mmol, 5.66 g) were added in small quantities, which caused the almost colorless organic layer to turn yellow. After 90 min of stirring, the dark brown solution (due to a slight excess of iodine) was further diluted with 20 mL of diethyl ether. To remove the excess of iodine, the mixture was transferred to a separatory funnel, and washed twice with 70 mL of 5 wt% sodium thiosulfate solution and once with 70 mL of deionized water. The orange-red organic layer was collected and dried over magnesium sulfate, after which it was filtered and concentrated *in vacuo* to yield the intermediate product (**1**) as a dark red oil (yield: 4.70 g, 78.8%), which was characterized by ^{1}H NMR (Figure 3.4) and used without further purification.

^{1}H NMR (400 MHz, $CDCl_3$): δ (ppm) = 1.02 (t, CH_3), 1.75 (sextet, CH_2), 3.29 (t, CH_2).

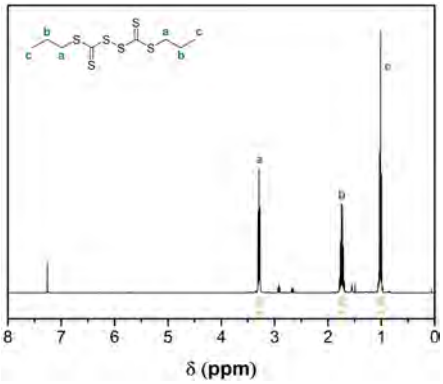

Figure 3.4. ^{1}H NMR spectrum ($CDCl_3$) of the intermediate, bis(propylsulfanylthiocarbonyl) disulfide (**1**).

The final product (**2**) was obtained in the second step of this procedure. Under nitrogen atmosphere, the intermediate (**1**) (1 eq., 14.9 mmol, 4.51 g), azobisisobutyronitrile (AIBN) (1.5 eq., 22.4 mmol, 3.68 g), and 60 mL of ethyl acetate were charged in a 250 mL three-neck round-bottom flask, equipped with a stirring bar, two stoppers, and a tap connected to nitrogen. The clear orange reaction mixture was deoxygenated via three freeze-pump-thaw cycles, after which it was immersed in a thermostated oil bath at 70 °C while stirring continuously. After 17 hours, the ethyl acetate was carefully removed *in vacuo* and the resulting orange suspension was separated from the excess AIBN and its decomposition product (tetramethylsuccinonitrile) via an extraction with 25 mL *n*-hexane and subsequent filtering. The *n*-hexane was subsequently removed *in vacuo* to yield an orange oil (5.65 g), which was characterized by ^{1}H NMR and TLC (R_f = 0.30), and further purified by silica gel column chromatography using *n*-hexane/ethyl acetate (20:1) as the eluent. The final product (**2**) was obtained as a bright orange oil (yield: 3.20 g, 49.1%), which was characterized by ^{1}H NMR (Figure 3.5a) and ^{13}C NMR (Figure 3.5b), and stored in the fridge until further use.

^{1}H NMR (400 MHz, $CDCl_3$): δ (ppm) = 1.02 (t, CH_3), 1.75 (sextet, CH_2), 1.87 (s, 2 CH_3), 3.32 (t, CH_2).

^{13}C NMR (100 MHz, $CDCl_3$): δ (ppm) = 13.6, 21.4, 27.2, 38.8, 42.5, 120.6, 217.9.

According to the ^{1}H NMR and ^{13}C NMR spectra (Figure 3.5), the RAFT agent was successfully synthesized in high purity.

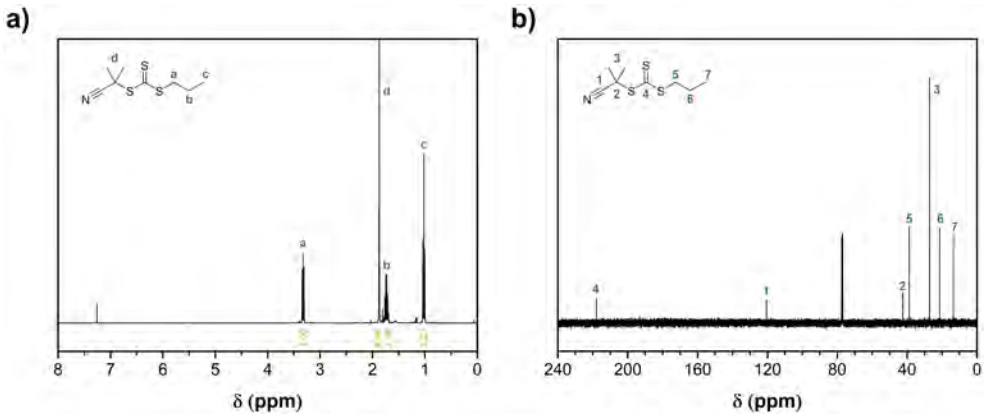

Figure 3.5. (a) ^{1}H NMR and (b) ^{13}C NMR spectra ($CDCl_3$) of the final product, CPP-TTC (**2**).

3.4.2. Synthesis of PS Macro-CTAs

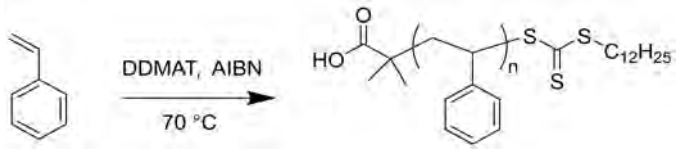

Scheme 3.2. Reaction scheme for the synthesis of PS macro-CTAs.

Polystyrene macro-CTAs were synthesized according to an adapted literature procedure.[39] The reaction conditions for obtaining PS macro-CTAs with distinct lengths are summarized in Table 3.1. Purified styrene, DDMAT, and AIBN were charged in a 25 mL round-bottom flask, equipped with a stirring bar and septum. Once all chemicals were dissolved, the yellow reaction mixture was sparged with nitrogen for 10 min. The flask was immersed in a thermostated oil bath at 70 °C while stirring continuously. After the indicated reaction time, the reaction mixture was quenched by cooling the flask in cold water and subsequently exposing it to air. A ^{1}H NMR sample was prepared in order to calculate the conversion through comparison of the monomer and polymer peaks. The viscous yellow polymer mixture was diluted with a small amount of THF (~2 mL) and precipitated dropwise into a beaker containing 500 mL of thoroughly stirred methanol. The precipitated product was collected by vacuum filtration, washed with methanol, and air-dried on the filter for at least an hour. The polymer product was redissolved in THF and the precipitation procedure was repeated. The purified polymer was collected and dried in a vacuum oven (40 °C) overnight. The yield of the yellow powder was determined and the product was characterized by ^{1}H NMR (Figure 3.6a), GPC (Figure 3.6b), and ATR-FTIR (Figure 3.8b).

^{1}H NMR (400 MHz, $CDCl_3$): δ (ppm) = 7.30–6.30 (br, 5 CH, aromatic ring), 3.26 (br, S-CH_2, CTA), 2.30–1.70 (br, CH), 1.70–1.30 (br, CH_2), 1.27 (br, $C_{10}H_{20}$, CTA), 0.89 (br, CH_3, CTA).

The PS macro-CTAs were successfully synthesized in high purity, as evidenced by ^{1}H NMR (Figure 3.6a). The single Gaussian-shaped peaks seen in GPC and the associated low dispersities (close to 1.1) indicate the synthesis of polymer chains of uniform length (Figure 3.6b). Unfortunately, the slow kinetics of the polymerization reaction prevented the facile and high-quality synthesis of high molecular weight polymers.

Table 3.1. Reaction conditions for the synthesis of PS macro-CTAs by RAFT polymerization. The subscripts denote the degree of polymerization. Amounts are given in mmol. Reaction times (t_R) are in hours, conversions were determined by ^{1}H NMR (%), yields are given in %, and molecular weights (M_n) are reported in kg mol^{-1}. $M_{n,calc}$ represents the calculated molecular weight based on the initial concentrations and monomer conversion. $M_{n,GPC}$ and the molecular weight distribution ($Đ$) were determined by GPC.

Polymer	Styrene	DDMAT	AIBN	t_R	Conv.	Yield	$M_{n,calc}$	$M_{n,GPC}$	$Đ$
PS_{27}	261 (96 eq.)	2.7 (1 eq.)	0.36 (0.13 eq.)	7	28.2	90.8	3.2	3.2	1.14
PS_{32}	39.9 (36 eq.)	1.1 (1 eq.)	0.12 (0.11 eq.)	18	87.9	76.2	3.7	3.5	1.10
PS_{47}	34.9 (62 eq.)	0.56 (1 eq.)	0.065 (0.12 eq.)	18	74.8	70.1	5.3	4.9	1.08
PS_{55}	20.9 (75 eq.)	0.28 (1 eq.)	0.032 (0.11 eq.)	18	72.8	36.0	6.1	5.4	1.07
PS_{81}	36.7 (135 eq.)	0.27 (1 eq.)	0.031 (0.11 eq.)	23	60.3	52.0	8.8	8.1	1.09
PS_{85}	36.7 (136 eq.)	0.27 (1 eq.)	0.031 (0.11 eq.)	22	63.3	49.4	9.2	8.3	1.09
PS_{87}	36.7 (136 eq.)	0.27 (1 eq.)	0.031 (0.11 eq.)	22	64.9	77.4	9.4	8.6	1.09
PS_{90}	36.7 (136 eq.)	0.27 (1 eq.)	0.031 (0.11 eq.)	23.5	67.1	76.8	9.7	8.4	1.09

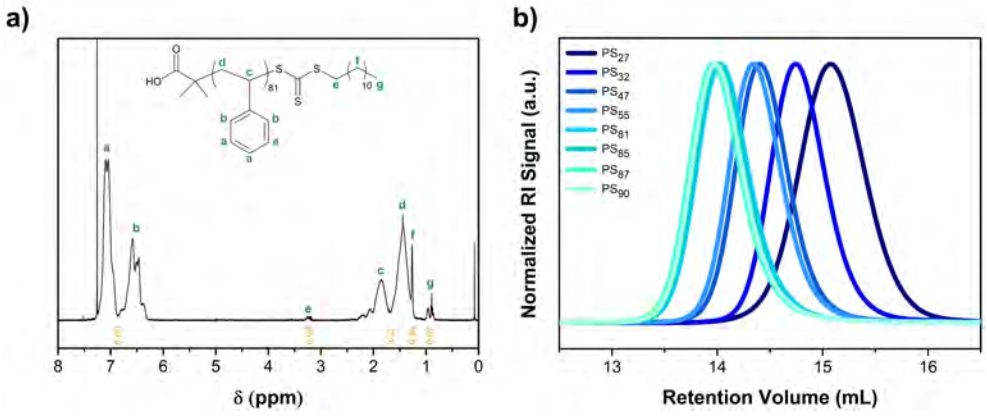

Figure 3.6. (a) ^{1}H NMR spectrum ($CDCl_3$) of a typical PS macro-CTA (PS_{81}). (b) GPC chromatograms (DMF) of all synthesized PS macro-CTAs: PS_{27}, PS_{32}, PS_{47}, PS_{55}, PS_{81}, PS_{85}, PS_{87}, and PS_{90}.

3.4.3. Synthesis of PS-*b*-PAA Diblock Copolymers

1. RAFT Synthesis of PS-*b*-P*t*BA

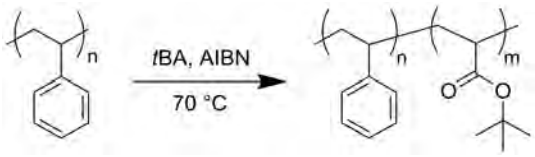

Scheme 3.3. Reaction scheme for the synthesis of PS-*b*-P*t*BA diblock copolymers.

The reaction conditions for obtaining PS-*b*-P*t*BA diblock copolymers with distinct block ratios and lengths are summarized in Table 3.2. PS macro-CTA, purified *tert*-butyl acrylate (*t*BA), AIBN (using a 1.0 mg mL^{-1} stock solution in 1,4-dioxane/anisole/THF), and 1,4-dioxane/anisole/THF were charged in a 20 mL glass vial and mixed until everything was dissolved. After complete dissolution, the yellow mixture was carefully transferred to a 25 mL round-bottom flask, equipped with a stirring bar and septum. The reaction mixture was sparged with nitrogen for 10 min. The flask was immersed in a thermostated oil bath at 70 °C. After the indicated reaction time, the reaction mixture was quenched by cooling the flask in cold water and subsequently exposing it to air. A ^{1}H NMR sample was prepared in order to calculate the conversion through comparison of the polystyrene and *t*BA peaks. The viscous yellow polymer mixture was purified by precipitating the undiluted solution into 500 mL of thoroughly stirred methanol. The precipitated product was collected by vacuum filtration, washed with methanol, air-dried on the filter, and further dried in a vacuum oven (40 °C) overnight. The yield of the slightly yellow powder was determined and the product was characterized by ^{1}H NMR (Figure 3.7a), GPC (Figure 3.7b and Figure A2), and ATR-FTIR (Figure 3.8b).

^{1}H NMR (400 MHz, $CDCl_3$): 7.30–6.30 (br, 5 CH, PS aromatic ring), 3.33 (br, S-CH_2, CTA), 2.35–1.10 (br, CH and CH_2, backbone PS and P*t*BA), 1.44 (s, -$C(CH_3)_3$, P*t*BA), 1.26 (br, $C_{10}H_{20}$, CTA), 0.90 (br, CH_3, CTA).

The PS-*b*-P*t*BA diblock copolymers were successfully synthesized in high purity, as evidenced by ^{1}H NMR (Figure 3.7a). GPC showed a clear shift to lower retention volumes indicative of a successful chain extension, albeit with somewhat higher dispersities than were initially recorded for the PS macro-CTAs (Figure 3.7b). The almost perfect alignment of the GPC curves of the PS_{81}-*b*-P*t*BA_{79}, PS_{81}-*b*-P*t*BA_{81}, and PS_{85}-*b*-P*t*BA_{81} diblock copolymers demonstrates the high reproducibility of the employed RAFT technique. The shoulders seen at lower retention volumes suggest the occurrence of chain-chain coupling. Finally, comparison of the ATR-FTIR spectra also confirmed the successful addition of the P*t*BA block, evidenced by the emerging characteristic absorption bands of P*t*BA: the -$C(CH_3)_3$ stretch at 1366 cm^{-1}, and the strong C=O (1724 cm^{-1}) and C-O (1144 cm^{-1}) stretching vibrations (Figure 3.8b).

Table 3.2. Reaction conditions for the synthesis of PS-*b*-P*t*BA diblock copolymers by RAFT polymerization. The subscripts denote the degree of polymerization of each block. Amounts of reactants are given in mmol and solvents in mL. Reaction times (t_R) are in hours, conversions were determined by ^{1}H NMR (%), yields are given in %, and molecular weights (M_n) are reported in kg mol^{-1}. f_{PtBA} represents the weight fraction of P*t*BA and $M_{n,calc}$ is the sum of the calculated molecular weights based on the initial concentrations and monomer conversion ($M_{n,PS}$ + $M_{n,PtBA}$). $M_{n,GPC}$ and the molecular weight distribution ($Đ$) were determined by GPC.

Polymer	PS-CTA	*t*BA	AIBN	Solvent	t_R	Conv.	Yield	f_{PtBA}	$M_{n,calc}$	$M_{n,GPC}$	$Đ$
PS_{32}-*b*-P*t*BA_{100}	0.14 (1 eq.)	14.4 (104 eq.)	0.012 (0.086 eq.)	5.0 (dioxane)	21	95.9	72.9	0.79	16.5	12.4	1.27
PS_{32}-*b*-P*t*BA_{277}	0.083 (1 eq.)	23.9 (288 eq.)	0.0072 (0.087 eq.)	8.1 (dioxane)	19	96.2	75.4	0.91	39.1	21.3	1.53
PS_{27}-*b*-P*t*BA_{287}	0.047 (1 eq.)	23.5 (499 eq.)	0.0049 (0.11 eq.)	10.3 (anisole)	6	57.7	8.2	0.93	40.0	29.8	1.20
PS_{27}-*b*-P*t*BA_{338}	0.063 (1 eq.)	27.7 (440 eq.)	0.0061 (0.10 eq.)	10.0 (dioxane)	5.5	76.4	55.6	0.94	46.5	39.0	1.30
PS_{27}-*b*-P*t*BA_{436}	0.047 (1 eq.)	23.4 (499 eq.)	0.0049 (0.11 eq.)	7.7 (THF)	23	87.2	14.5	0.95	59.1	31.5	1.79
PS_{81}-*b*-P*t*BA_{79}	0.038 (1 eq.)	3.10 (81 eq.)	0.0042 (0.11 eq.)	1.1 (dioxane)	23	96.2	62.3	0.55	18.9	15.1	1.17
PS_{81}-*b*-P*t*BA_{81}	0.10 (1 eq.)	8.55 (82 eq.)	0.012 (0.12 eq.)	2.9 (dioxane)	22	98.8	56.6	0.55	19.2	15.6	1.15
PS_{85}-*b*-P*t*BA_{81}	0.12 (1 eq.)	9.75 (82 eq.)	0.013 (0.11 eq.)	3.3 (dioxane)	23	99.4	79.3	0.54	19.6	15.8	1.15

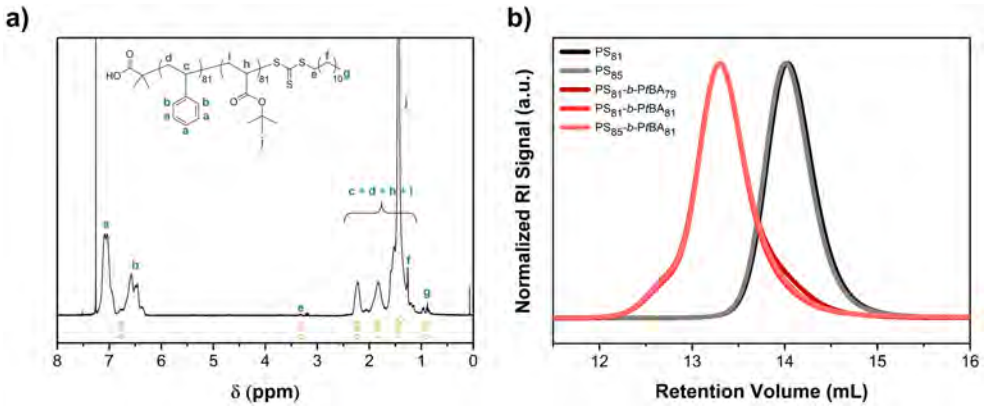

Figure 3.7. (a) ^{1}H NMR spectrum ($CDCl_3$) of a typical PS-*b*-P*t*BA diblock copolymer (PS_{81}-*b*-$PtBA_{81}$). (b) GPC chromatograms (DMF) of the $PS_{81/85}$ macro-CTAs (black) and the $PS_{81/85}$-*b*-P*t*$BA_{79/81}$ diblock copolymers (red).

2. Deprotection of PS-*b*-P*t*BA

1. HFIP/HCl

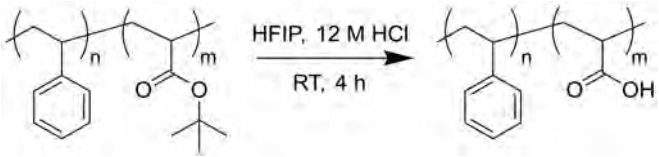

Scheme 3.4. Reaction scheme for the deprotection of PS-*b*-P*t*BA diblock copolymers containing a short PS block.

The deprotection of PS-*b*-P*t*BA diblock copolymers containing a short PS block (PS_{27} and PS_{32}) was performed according to a previously reported procedure.[40]

PS-*b*-P*t*BA (1 g, 1 eq. *t*BA) was charged in a 250 mL round-bottom flask and dissolved in 100 to 130 mL of 1,1,1,3,3,3-hexafluoro-2-propanol (HFIP). Once dissolved, 12 M HCl (1.3 eq.) was added dropwise to the stirred polymer solution. After 4 hours, the solvent was removed *in vacuo* and the obtained product was redissolved in THF (8–10 mL) and precipitated into 500 mL of stirred *n*-pentane. The precipitated product was collected by vacuum filtration, redissolved in THF, and the precipitation procedure was repeated. The purified polymer was collected and dried in a vacuum oven (40 °C) overnight. The yield of the slightly yellow powder was determined (88–93%) and the product was characterized by ^{1}H NMR (Figure 3.8a) and ATR-FTIR (Figure 3.8b).

^{1}H NMR (400 MHz, DMSO-d_6): δ (ppm) = 12.22 (s, COOH), 7.40–6.10 (br, 5 CH, PS aromatic ring), 2.40–1.00 (br, CH and CH_2, backbone PS and PAA).

2. Dioxane/HCl + reflux

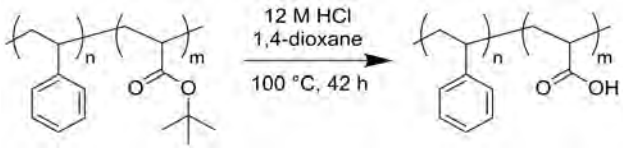

Scheme 3.5. Reaction scheme for the deprotection of PS-*b*-P*t*BA diblock copolymers containing a long PS block.

Due to the insolubility of long PS blocks in HFIP, a different deprotection method was followed for the $PS_{81/85}$-containing diblock copolymers.[41,42]

PS-*b*-P*t*BA (1 g, 1 eq. *t*BA) was dissolved in 12 mL of 1,4-dioxane in a 50 mL round-bottom flask, equipped with a stirring bar and a reflux condenser. After dissolution, 12 M HCl (5 eq.) was added to the stirred solution and the mixture was heated to 100 °C. After 42 hours, the mixture was cooled down, the solvent was removed *in vacuo*, and a ^{1}H NMR spectrum was recorded to confirm the successful deprotection. The deprotected polymer was redissolved in 10 mL of 1,4-dioxane and precipitated into 500 mL of stirred *n*-pentane. The precipitated brownish powder was collected by vacuum filtration and dried in a vacuum oven (40 °C) overnight. The yield of the light brown powder was determined (88%) and the product was characterized by ^{1}H NMR (Figure 3.8a) and ATR-FTIR (Figure 3.8b). The trithiocarbonate end-groups were not affected by the employed deprotection conditions, as evidenced by ^{1}H NMR (Figure 3.9a) and GPC (Figure 3.9b).

^{1}H NMR (400 MHz, DMSO-d_6): δ (ppm) = 12.22 (s, COOH), 7.40–6.10 (br, 5 CH, PS aromatic ring), 2.40–1.00 (br, CH and CH_2, backbone PS and PAA).

Besides solvent impurities (i.e., 1,4-dioxane and DMF), the PS-*b*-P*t*BA diblock copolymers were successfully deprotected to give PS-*b*-PAA, as evidenced by the emerging carboxylic acid peak (12.2 ppm) and disappearing *tert*-butyl peak (1.44 ppm) in ^{1}H NMR (Figure 3.8a). Comparison of the ATR-FTIR spectra also confirmed the successful conversion into PS-*b*-PAA, marked by the absence of the -$C(CH_3)_3$ and C-O stretching vibrations as well as the broadening of the C=O stretching vibration (1724 cm^{-1}) (Figure 3.8b). Characterization by GPC was discouraged due to undesired interactions between the charged polymer and the GPC column.

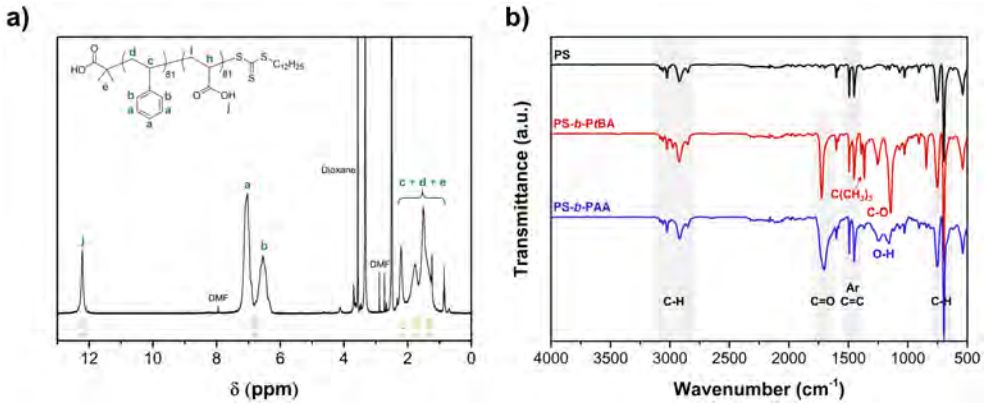

Figure 3.8. (a) ^{1}H NMR spectrum (DMSO-d_6) of a typical PS-*b*-PAA diblock copolymer (PS_{81}-*b*-PAA_{81}). (b) ATR-FTIR spectra of the synthesized PS_{81} macro-CTA (black) and the PS_{81}-*b*-P*t*BA_{81} (red) and PS_{81}-*b*-PAA_{81} (blue) diblock copolymers.

The incorporated RAFT end-groups were not affected by the employed dioxane/HCl deprotection conditions, demonstrated by the still-present ^{1}H NMR signals of the CTA and the unchanged GPC signal of PS-CTA after performing the deprotection protocol (Figure 3.9). Hence, thiol end-groups were not formed through trithiocarbonate hydrolysis, as this would have promoted disulfide bridge formation (i.e., chain-chain coupling), leading to a doubling of the molecular weight.

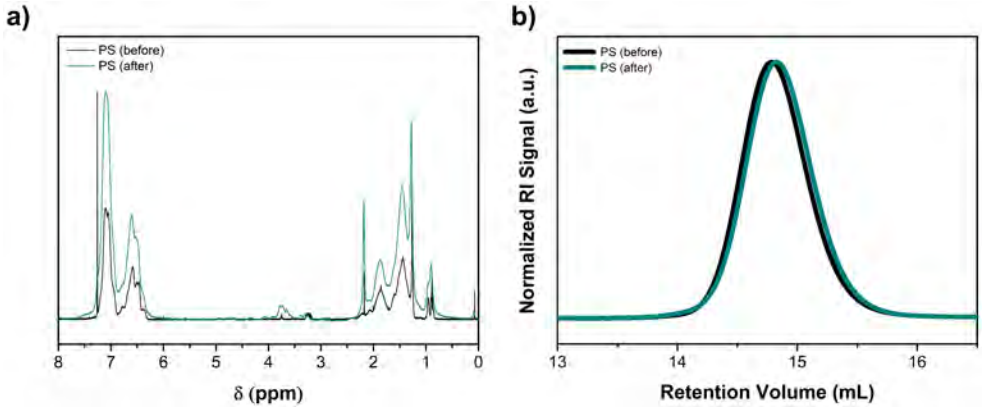

Figure 3.9. (a) ^{1}H NMR spectra ($CDCl_3$) and (b) GPC chromatograms (DMF) of the control experiment: PS_{32} macro-CTA before (black) and after (green) performing the 42 h dioxane/HCl reflux deprotection protocol.

3.4.4. Synthesis of PMMA Macro-CTAs

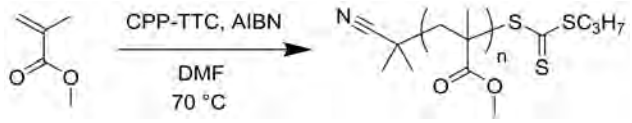

Scheme 3.6. Reaction scheme for the synthesis of PMMA macro-CTAs.

PMMA macro-CTAs were synthesized according to a previously reported procedure.[38] The reaction conditions for obtaining PMMA macro-CTAs with distinct lengths are summarized in Table 3.3. Purified methyl methacrylate (MMA), CPP-TTC, AIBN (using a stock solution in DMF), and DMF were charged in a 50 mL round-bottom flask, equipped with a stirring bar and septum. Once all chemicals were dissolved, the bright yellow reaction mixture was sparged with nitrogen for 30 min. The flask was immersed in a thermostated oil bath at 70 °C while stirring continuously. After 20 to 21 hours, the reaction mixture was quenched by cooling the flask in cold water and subsequently exposing it to air. A ^{1}H NMR sample was prepared in order to calculate the conversion through comparison of the monomer and polymer peaks. The undiluted yellow polymer mixture was purified by precipitation into 300 mL *n*-hexane/ethanol (2:1). The precipitated product was collected by vacuum filtration (using a glass filter), washed with *n*-hexane, and air-dried on the filter for at least an hour. The polymer product was subsequently redissolved in acetone and re-precipitated in 300 mL *n*-hexane/ethanol (2.5:1), filtered using a glass filter, washed with *n*-hexane, and finally dried in a vacuum oven (40 °C) overnight. The yield of the fine off-white powder was determined and the product was characterized by ^{1}H NMR (Figure 3.10a), GPC (Figure 3.10b), and ATR-FTIR (Figure 3.12b).

^{1}H NMR (400 MHz, $CDCl_3$): δ (ppm) = 3.59 (s, O-CH_3), 3.22 (t, S-CH_2, CTA), 2.2–1.1 (br, CH_2), 1.1–0.7 (br, CH_3).

The PMMA macro-CTAs were successfully synthesized in high purity, as evidenced by ^{1}H NMR (Figure 3.10a). The calculated molecular weights (M_n) based on ^{1}H NMR match the values recorded by GPC rather well. The single Gaussian-shaped peaks seen in GPC are characterized by relatively low dispersities, although the slightly asymmetrical peak shape (i.e., tailing) of the higher molecular weight polymers may be indicative of a slow initiation (with respect to propagation) and/or premature termination (Figure 3.10b). Unfortunately, similarly to the PS macro-CTAs, the slow kinetics of the polymerization reaction prevented the facile and high-quality synthesis of high molecular weight polymers.

Table 3.3. Reaction conditions for the synthesis of PMMA macro-CTAs by RAFT polymerization. The subscripts denote the degree of polymerization. Amounts of reactants are given in mmol and solvents in mL. Reaction times (t_R) are in hours, conversions were determined by ^{1}H NMR (%), yields are given in %, and molecular weights (M_n) are reported in kg mol^{-1}. $M_{n,calc}$ represents the calculated molecular weight based on the initial concentrations and monomer conversion. $M_{n,GPC}$ and the molecular weight distribution ($Đ$) were determined by GPC.

Polymer	MMA	CPP-TTC	AIBN	DMF	t_R	Conv.	Yield	$M_{n,calc}$	$M_{n,GPC}$	$Đ$
$PMMA_{31}$	30.7 (40 eq.)	0.77 (1 eq.)	0.010 (0.012 eq.)	5.4	21	77.8	47.6	3.3	4.7	1.18
$PMMA_{45}$	40.3 (60 eq.)	0.68 (1 eq.)	0.013 (0.019 eq.)	7.2	21	76.3	65.6	4.8	6.5	1.20
$PMMA_{80}$	50.0 (110 eq.)	0.45 (1 eq.)	0.016 (0.035 eq.)	10.7	20	71.4	73.9	8.2	9.8	1.24
$PMMA_{90}$	49.9 (111 eq.)	0.45 (1 eq.)	0.016 (0.035 eq.)	8.9	20	80.8	74.1	9.2	9.3	1.26
$PMMA_{207}$	60.8 (247 eq.)	0.25 (1 eq.)	0.016 (0.065 eq.)	9.5	21	83.6	81.1	21.0	18.1	1.25
$PMMA_{486}$	54.8 (575 eq.)	0.095 (1 eq.)	0.017 (0.18 eq.)	9.0	20	84.4	73.8	48.9	32.8	1.40

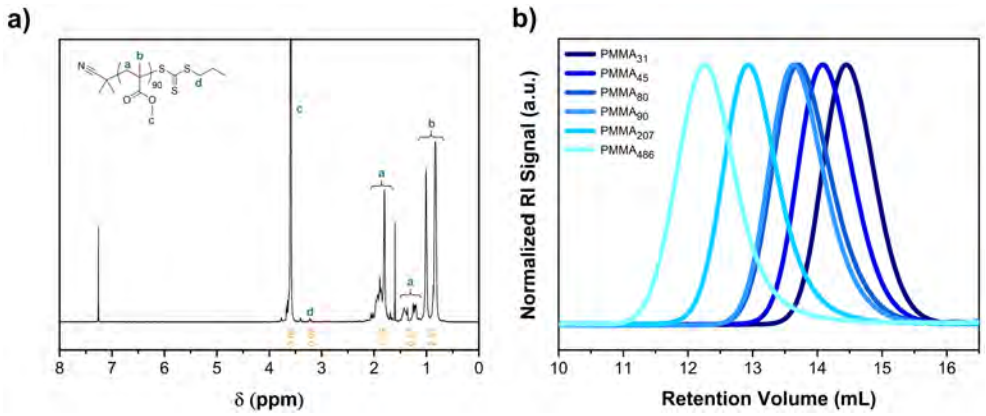

Figure 3.10. (a) ^{1}H NMR spectrum ($CDCl_3$) of a typical PMMA macro-CTA ($PMMA_{90}$). (b) GPC chromatograms (DMF) of all synthesized PMMA macro-CTAs: $PMMA_{31}$, $PMMA_{45}$, $PMMA_{80}$, $PMMA_{90}$, $PMMA_{207}$, and $PMMA_{486}$.

3.4.5. Synthesis of PMMA-*b*-PAA Diblock Copolymers

1. RAFT Synthesis of PMMA-*b*-P*t*BA

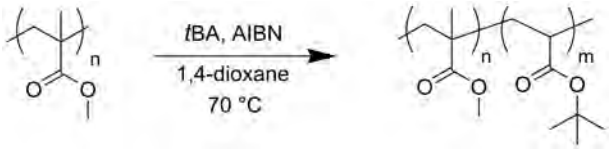

Scheme 3.7. Reaction scheme for the synthesis of PMMA-*b*-P*t*BA diblock copolymers.

The reaction conditions for obtaining PMMA-*b*-P*t*BA diblock copolymers with distinct block ratios and lengths are summarized in Table 3.4. PMMA macro-CTA, purified *t*BA, AIBN (using a stock solution in 1,4-dioxane), and 1,4-dioxane were charged in a 50 mL round-bottom flask, equipped with a stirring bar and septum. The reaction mixture was sparged with nitrogen for 20 min. The flask was immersed in a thermostated oil bath at 70 °C. After the indicated reaction time, the reaction mixture was quenched by cooling the flask in cold water and subsequently exposing it to air. A ^{1}H NMR sample was prepared in order to calculate the conversion through comparison of the *t*BA and P*t*BA peaks. The viscous yellow polymer mixture was diluted with a small amount of methanol and precipitated dropwise into 500 mL of thoroughly stirred deionized water. The precipitated product was collected by vacuum filtration over a glass filter and dried in a vacuum oven (40 °C) overnight. The yield of the slightly yellowish powder was determined and the product was characterized by ^{1}H NMR (Figure 3.11a), GPC (Figure 3.11b and Figure A3), and ATR-FTIR (Figure 3.12b).

^{1}H NMR (400 MHz, $CDCl_3$): 3.59 (s, O-CH_3, PMMA), 2.22 (br, CH, P*t*BA), 2.1–1.5 (br, CH_2, PMMA and P*t*BA), 1.43 (s, 3x CH_3, P*t*BA), 1.01–0.84 (br, CH_3, PMMA).

The PMMA-*b*-P*t*BA diblock copolymers were successfully synthesized with notably high conversions and in high purity, as evidenced by ^{1}H NMR (Figure 3.11a). GPC showed a clear shift to lower retention volumes indicative of a successful chain extension, albeit with somewhat higher dispersities than were initially recorded for the PMMA macro-CTAs (Figure 3.11b). The relatively high dispersities ($Đ$ > 1.4) as well as the slight shoulders seen at lower retention volumes (i.e., chain-chain coupling), are the result of long reaction times, which increases the probability of termination with respect to propagation. The almost perfect alignment of the GPC curves of $PMMA_{90}$-*b*-P*t*BA_{113} and $PMMA_{90}$-*b*-P*t*BA_{184} can be explained by a similarity in polymer coil dimensions when dissolved in DMF. Finally, comparison of the ATR-FTIR spectra also confirmed the successful addition of the P*t*BA block, evidenced by the emerging characteristic -$C(CH_3)_3$ stretching vibration of P*t*BA at 1366 cm^{-1} (Figure 3.12b).

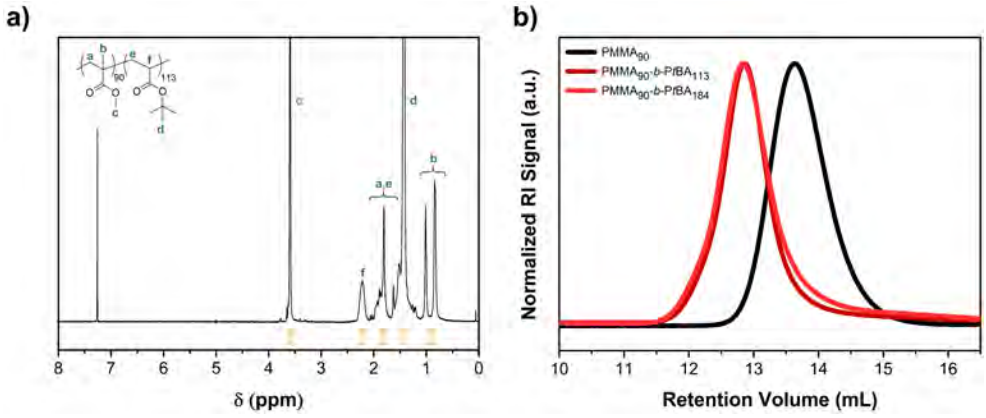

Figure 3.11. (a) ^{1}H NMR spectrum ($CDCl_3$) of a typical PMMA-*b*-P*t*BA diblock copolymer ($PMMA_{90}$-*b*-P*t*BA_{113}). (b) GPC chromatograms (DMF) of the $PMMA_{90}$ macro-CTA (black) and the $PMMA_{90}$-*b*-P*t*BA_x diblock copolymers (red).

Table 3.4. Reaction conditions for the synthesis of PMMA-*b*-P*t*BA diblock copolymers by RAFT polymerization. The subscripts denote the degree of polymerization of each block. Amounts of reactants are given in mmol and solvents in mL. Reaction times (t_R) are in hours, conversions were determined by ^{1}H NMR (%), yields are given in %, and molecular weights (M_n) are reported in kg mol^{-1}. f_{PtBA} represents the weight fraction of P*t*BA and $M_{n,calc}$ is the sum of the calculated molecular weights based on the initial concentrations and monomer conversion ($M_{n,PMMA} + M_{n,PtBA}$). $M_{n,GPC}$ and the molecular weight distribution ($Đ$) were determined by GPC.

Polymer	PMMA-CTA	*t*BA	AIBN	Dioxane	t_R	Conv.	Yield	f_{PtBA}	$M_{n,calc}$	$M_{n,GPC}$	$Đ$
$PMMA_{31}$-*b*-$PtBA_{114}$	0.14 (1 eq.)	15.6 (115 eq.)	0.010 (0.074 eq.)	5.6	22	99.2	79.5	0.82	17.9	13.8	1.47
$PMMA_{45}$-*b*-$PtBA_{112}$	0.11 (1 eq.)	12.0 (113 eq.)	0.0078 (0.074 eq.)	4.3	21	98.7	77.6	0.76	19.1	15.7	1.41
$PMMA_{45}$-*b*-$PtBA_{186}$	0.063 (1 eq.)	11.9 (188 eq.)	0.0076 (0.12 eq.)	4.2	20	98.6	77.3	0.84	28.9	21.1	1.44
$PMMA_{80}$-*b*-$PtBA_{118}$	0.22 (1 eq.)	26.2 (118 eq.)	0.020 (0.090 eq.)	7.4	18	98.8	94.4	0.65	23.2	18.9	1.40
$PMMA_{90}$-*b*-$PtBA_{113}$	0.19 (1 eq.)	21.9 (114 eq.)	0.014 (0.073 eq.)	7.7	18	98.9	78.6	0.62	23.6	17.4	1.46
$PMMA_{90}$-*b*-$PtBA_{184}$	0.056 (1 eq.)	10.3 (186 eq.)	0.0067 (0.12 eq.)	4.7	23	99.1	81.2	0.72	32.8	21.0	1.42

2. Deprotection of PMMA-*b*-P*t*BA

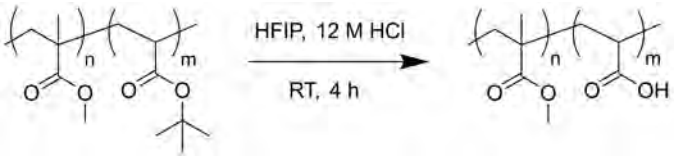

Scheme 3.8. Reaction scheme for the deprotection of PMMA-*b*-P*t*BA diblock copolymers.

The deprotection of all synthesized PMMA-*b*-P*t*BA diblock copolymers was performed according to the HFIP/HCl procedure.[40]

PMMA-*b*-P*t*BA (1 g, 1 eq. *t*BA) was charged in a 100 mL round-bottom flask and dissolved in 30 to 40 mL of HFIP. Once dissolved, 12 M HCl (1.3 eq.) was added dropwise to the stirred polymer solution. After 4 hours, the solvent was removed *in vacuo* and the obtained product was redissolved in 1,4-dioxane (10 mL) and precipitated into 500 mL of stirred *n*-pentane. The precipitated product was collected by vacuum filtration over a glass filter and dried in a vacuum oven (40 °C) overnight. The yield of the obtained slightly yellowish powder (93–98%) was determined and the product was characterized by ^{1}H NMR (Figure 3.12a) and ATR-FTIR (Figure 3.12b).

^{1}H NMR (400 MHz, DMSO-d_6): δ (ppm) = 12.23 (s, COOH), 3.56 (s, O-CH_3, PMMA), 2.20 (br, CH, PAA), 2.1–1.5 (br, CH_2, PMMA and PAA), 0.93–0.74 (br, CH_3, PMMA).

Besides minor solvent impurities (i.e., DMF), the PMMA-*b*-P*t*BA diblock copolymers were successfully deprotected to give PMMA-*b*-PAA, as evidenced by the emerging carboxylic acid peak (12.2 ppm) and disappearing *tert*-butyl peak (1.43 ppm) in ^{1}H NMR (Figure 3.12a). Comparison of the ATR-FTIR spectra also confirmed the successful conversion to PMMA-*b*-PAA, marked by the absence of the -$C(CH_3)_3$ stretch as well as a broadening of the absorption bands around 3000 cm^{-1} (-OH stretch) and 1724 cm^{-1} (C=O stretch) corresponding to the carboxylic acid group (Figure 3.12b). Characterization by GPC was discouraged due to undesired interactions between the charged polymer and the GPC column.

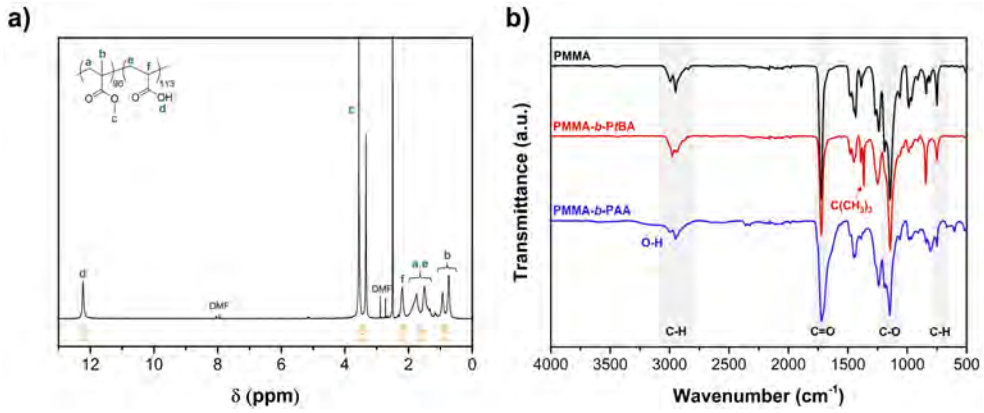

Figure 3.12. (a) ^{1}H NMR spectrum (DMSO-d_6) of a typical PMMA-*b*-PAA diblock copolymer ($PMMA_{90}$-*b*-PAA_{113}). (b) ATR-FTIR spectra of the synthesized $PMMA_{90}$ macro-CTA (black) and the $PMMA_{90}$-*b*-P*t*BA_{113} (red) and $PMMA_{90}$-*b*-PAA_{113} (blue) diblock copolymers.

3.4.6. Synthesis of PAA Homopolymers

1. RAFT Synthesis of P*t*BA

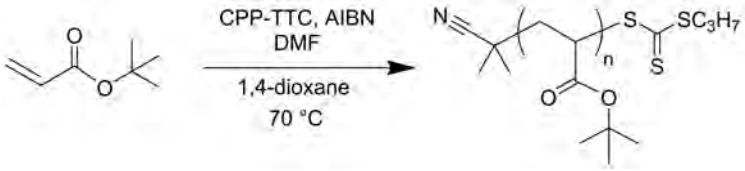

Scheme 3.9. Reaction scheme for the synthesis of P*t*BA homopolymers.

The reaction conditions for obtaining P*t*BA homopolymers with distinct lengths are summarized in Table 3.5.

Purified *t*BA, CPP-TTC, AIBN, 1,4-dioxane, and DMF were charged in a 100 mL round-bottom flask equipped with a stirring bar and septum. After complete dissolution, the reaction mixture was sparged with nitrogen for 10 min. A t = 0 h ^{1}H NMR sample was taken towards the end of the degassing cycle. The flask was immersed in a thermostated oil bath at 70 °C. After roughly 2 hours, the reaction mixture was quenched by cooling the flask in cold water and subsequently exposing it to air. A $t \approx 2$ h ^{1}H NMR sample was prepared in order to calculate the conversion through comparison of the DMF standard and *t*BA peaks. The yellow reaction mixture was purified by precipitation into 400 mL of cold methanol/deionized water (3:1). The precipitated product was collected by vacuum filtration and air-dried on the filter. The polymer product was redissolved in 1,4-dioxane and the precipitation procedure was repeated. The purified polymer was collected and dried in a vacuum oven (40 °C) overnight. The yield of the yellowish powder was determined and the product was

characterized by ^{1}H NMR (Figure 3.13a), GPC (Figure 3.13b), and ATR-FTIR (Figure 3.14b).

^{1}H NMR (400 MHz, $CDCl_3$): δ (ppm) = 3.31 (t, s-CH_2, CTA), 2.21 (br, CH, backbone), 1.95–1.15 (br, CH_2, backbone), 1.43 (s, -$C(CH_3)_3$).

The P*t*BA homopolymers were successfully synthesized in high purity, as evidenced by ^{1}H NMR (Figure 3.13a). The single Gaussian-shaped peaks seen in GPC are characterized by relatively low dispersities, although the slightly asymmetrical peak shape (i.e., tailing) seen for the higher molecular weight P*t*BA$_{142}$ polymer may be indicative of a slow initiation (with respect to propagation) and/or premature termination (Figure 3.13b). The almost perfect alignment of the GPC curves of P*t*BA$_{107}$ and P*t*BA$_{120}$ can be explained by a similarity in polymer coil dimensions when dissolved in DMF.

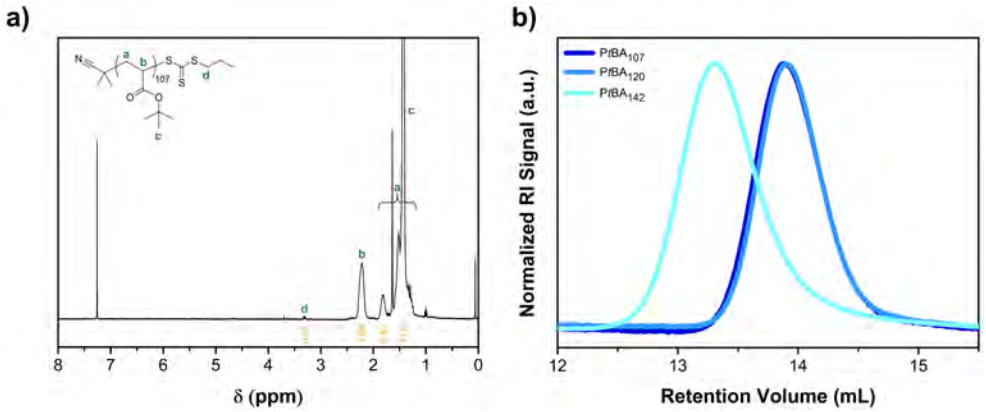

Figure 3.13. (a) ^{1}H NMR spectrum ($CDCl_3$) of a typical P*t*BA homopolymer (P*t*BA$_{107}$). (b) GPC chromatograms (DMF) of all synthesized P*t*BA homopolymers: P*t*BA$_{107}$, P*t*BA$_{120}$, and P*t*BA$_{142}$.

Table 3.5. Reaction conditions for the synthesis of P*t*BA homopolymers by RAFT polymerization. The subscripts denote the degree of polymerization. Amounts of reactants are given in mmol and solvents in mL. Reaction times (t_R) are in hours, conversions were determined by ^{1}H NMR (%), yields are given in %, and molecular weights (M_n) are reported in kg mol^{-1}. $M_{n,calc}$ represents the calculated molecular weight based on the initial concentrations and monomer conversion. $M_{n,GPC}$ and the molecular weight distribution ($Đ$) were determined by GPC.

Polymer	*t*BA	CPP-TTC	AIBN	DMF	Dioxane	t_R	Conv.	Yield	$M_{n,calc}$	$M_{n,GPC}$	$Đ$
P*t*BA$_{107}$	91.2 (200 eq.)	0.46 (1 eq.)	0.047 (0.1 eq.)	7.1	31.1	2	53.4	86.2	13.7	13.4	1.14
P*t*BA$_{120}$	9.12 (191 eq.)	0.048 (1 eq.)	0.0046 (0.1 eq.)	0.71	3.1	2.25	63.1	64.9	15.4	13.2	1.13
P*t*BA$_{142}$	9.15 (207 eq.)	0.044 (1 eq.)	0.0046 (0.1 eq.)	0.71	3.1	2.25	68.5	7.2	18.2	16.5	1.14

2. Deprotection of P*t*BA

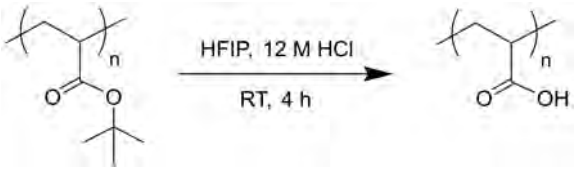

Scheme 3.10. Reaction scheme for the deprotection of P*t*BA homopolymers.

The deprotection of poly(*tert*-butyl acrylate) (P*t*BA) to give poly(acrylic acid) (PAA) was performed according to the HFIP/HCl procedure.[40]

P*t*BA polymer (1 g, 1 eq.) was charged in a 250 mL round-bottom flask and dissolved in 50 to 60 mL of HFIP. Once dissolved, 12 M HCl (1.3 eq.) was added dropwise to the stirred polymer solution. After 4 hours, the solvent was removed *in vacuo* and the obtained product was dissolved in ethanol and precipitated into 500 mL of *n*-pentane. The precipitated product was collected by vacuum filtration, redissolved in ethanol, and the precipitation procedure was repeated. The purified polymer was collected and dried in a vacuum oven (40 °C) overnight. The yield of the yellowish powder was determined (85–86%) and the product was characterized by ^{1}H NMR (Figure 3.14a) and ATR-FTIR (Figure 3.14b).

^{1}H NMR (400 MHz, DMSO-d_6): δ (ppm) = 12.23 (s, -OH), 2.20 (s, CH, backbone), 1.95–1.15 (br, CH_2, backbone).

Besides solvent impurities (i.e., ethanol), the P*t*BA homopolymers were successfully deprotected to give PAA, as evidenced by the emerging carboxylic acid peak (12.2 ppm) and disappearing *tert*-butyl peak (1.43 ppm) in ^{1}H NMR (Figure 3.14a). Comparison of the ATR-FTIR spectra also confirmed the successful conversion to PAA, marked by the absence of the -C(CH_3)$_3$ and C-O stretching vibrations as well as a broadening of the absorption bands around 3000 cm^{-1} (-OH stretch) and 1724 cm^{-1} (C=O stretch) corresponding to the carboxylic acid group (Figure 3.14b). Due to the unavailability of an aqueous GPC, and because of undesired interactions between the polymer and the GPC column when dissolved in DMF, characterization via GPC was not performed. However, the degree of polymerization is expected to be unaffected by the removal of the *tert*-butyl group.

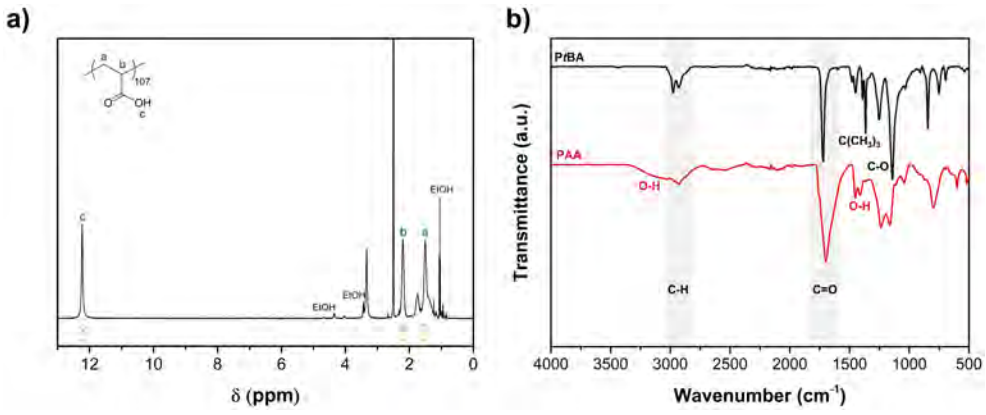

Figure 3.14. (a) ^{1}H NMR spectrum (DMSO-d_6) of a typical PAA homopolymer (PAA_{107}). (b) ATR-FTIR spectra of the synthesized $PtBA_{107}$ (black) and PAA_{107} (red) homopolymers.

3.4.7. Synthesis of the $PDMAEMA_{30}$ Macro-CTA

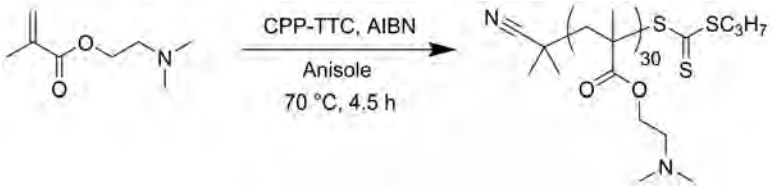

Scheme 3.11. Reaction scheme for the synthesis of the $PDMAEMA_{30}$ macro-CTA.

Purified 2-(dimethylamino)ethyl methacrylate (DMAEMA) (50 eq., 22.9 mmol, 3.59 g), CPP-TTC (1 eq., 0.461 mmol, 101 mg), AIBN (0.1 eq., 0.047 mmol, 7.7 mg), and anisole (9.9 mL) were charged in a 25 mL round-bottom flask equipped with a stirring bar and septum. After complete dissolution, the reaction mixture was sparged with argon for 15 min. A t = 0 h ^{1}H NMR sample was taken towards the end of the degassing cycle. The flask was immersed in a thermostated oil bath at 70 °C. After 4.5 hours, the reaction mixture was quenched by cooling the flask in cold water and subsequently exposing it to air. A t = 4.5 h ^{1}H NMR sample was prepared in order to calculate the conversion through comparison of the anisole standard and DMAEMA peaks (conv. = 61%). The reaction mixture was purified by precipitation into cold *n*-hexane, after which it was collected by vacuum filtration. The polymer product was redissolved in 1,4-dioxane and the precipitation procedure was repeated twice. The polymer was dried at room temperature under high vacuum overnight. The yield of the fine yellow powder was determined (1.67 g, 74.2%) and the product was characterized by ^{1}H NMR (Figure 3.15a), GPC (Figure 3.15b), and ATR-FTIR (Figure 3.17).

^{1}H NMR (400 MHz, $CDCl_3$): δ (ppm) = 4.06 (br, O-CH_2), 3.23 (t, S-CH_2, CTA), 2.56 (br, N-CH_2), 2.28 (s, 2x N-CH_3), 2.1–1.7 (br, CH_2, backbone), 1.2–0.7 (br, CH_3, backbone). Conversion = 61%, $M_{n,NMR}$ = 4.9 kg mol^{-1}, $P_{n,NMR}$ = 30.

GPC (DMF): $M_{n,GPC}$ = 7.2 kg mol^{-1}, $Đ$ = 1.17.

Besides minor solvent impurities (i.e., anisole), the PDMAEMA macro-CTA was successfully synthesized in high purity, as evidenced by ^{1}H NMR (Figure 3.15a). The single Gaussian-shaped peak seen in GPC and the associated low dispersity indicate the synthesis of polymer chains of uniform length (Figure 3.15b).

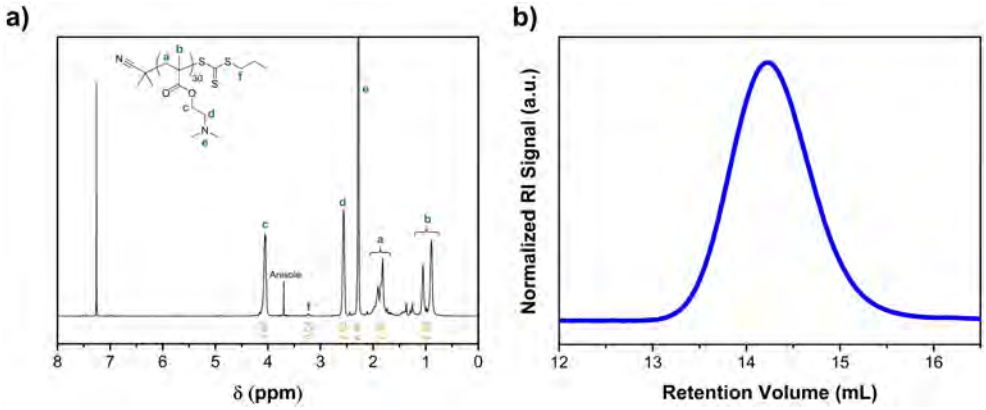

Figure 3.15. (a) ^{1}H NMR spectrum ($CDCl_3$) and (b) GPC chromatogram (DMF) of the $PDMAEMA_{30}$ macro-CTA.

3.4.8. Synthesis of $PDMAEMA_{30}$-*b*-$POEGMA_{97}$

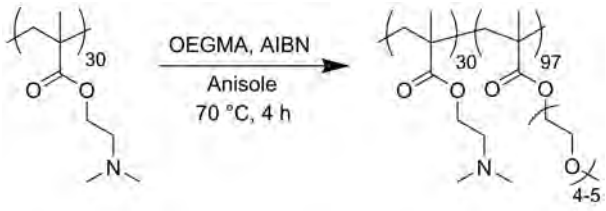

Scheme 3.12. Reaction scheme for the synthesis of the $PDMAEMA_{30}$-*b*-$POEGMA_{97}$ diblock copolymer.

$PDMAEMA_{30}$ macro-CTA (1 eq., 0.0407 mmol, 199 mg), oligo(ethylene glycol) methyl ether methacrylate (OEGMA) (166 eq., 6.75 mmol, 2.03 g), AIBN (0.1 eq., 0.0042 mmol, 0.70 mg – using 92 mg of a 7.6 mg mL^{-1} stock solution in anisole), and anisole (800 eq., 5.76 mL) were charged in a 25 mL round-bottom flask equipped with a stirring bar and septum. After complete dissolution, the reaction mixture was sparged with argon for 10 min. A t = 0 h ^{1}H NMR sample was taken towards the end of the degassing cycle. The flask was immersed in a thermostated oil bath at 70 °C. After 4 hours, the reaction mixture was quenched by cooling the flask in cold water and subsequently exposing it to air. A t = 4 h ^{1}H NMR sample was prepared in order to calculate the conversion through comparison of the anisole standard and OEGMA peaks (conv. = 55%). The

reaction mixture was purified by precipitation into cold *n*-hexane, after which it was collected by vacuum filtration. The polymer product was redissolved in acetone and the precipitation procedure was repeated twice. The polymer was dried at room temperature under high vacuum overnight. The yield of the yellow soft solid was determined (1.24 g, 99%) and the product was characterized by ^{1}H NMR (Figure 3.16a), GPC (Figure 3.16b), and ATR-FTIR (Figure 3.17).

^{1}H NMR (400 MHz, $CDCl_3$): δ (ppm) = 4.08 (br, COO-CH_2), 3.65 (br, CH_2, POEGMA), 3.55 (br, CH_2, POEGMA), 3.38 (s, O-CH_3, POEGMA), 2.56 (br, CH_2-N PDMAEMA), 2.28 (s, N-$(CH_3)_2$, PDMAEMA), 2.1–1.5 (br, CH_2, backbone), 1.2–0.5 (br, CH_3, backbone). Conversion = 55%, $M_{n,POEGMA}$ = 29.1 kg mol^{-1}, $P_{n,POEGMA}$ = 97. $M_{n,total}$ = 34.0 kg mol^{-1}. x_{POEGMA} = 0.764, f_{POEGMA} = 0.861.

GPC (DMF): $M_{n,GPC}$ = 23.0 kg mol^{-1}, $Đ$ = 1.28.

The PDMAEMA-*b*-POEGMA diblock copolymer was successfully synthesized in high purity, as evidenced by ^{1}H NMR (Figure 3.16a). The conversion of this bulky polymer was deliberately kept low to avoid chain-chain coupling.[43] Due to the presence of many identical characteristic groups in PDMAEMA and POEGMA (i.e., identical IR absorption bands), it was difficult to conclude the successful addition of the POEGMA block based on ATR-FTIR (Figure 3.17). However, GPC showed a clear shift to lower retention volumes indicative of a successful chain extension, albeit with a somewhat higher dispersity than was initially recorded for the PDMAEMA macro-CTA (Figure 3.16b). The observed slightly asymmetrical peak shape (i.e., tailing) is indicative of a slow initiation (with respect to propagation) and/or premature termination.

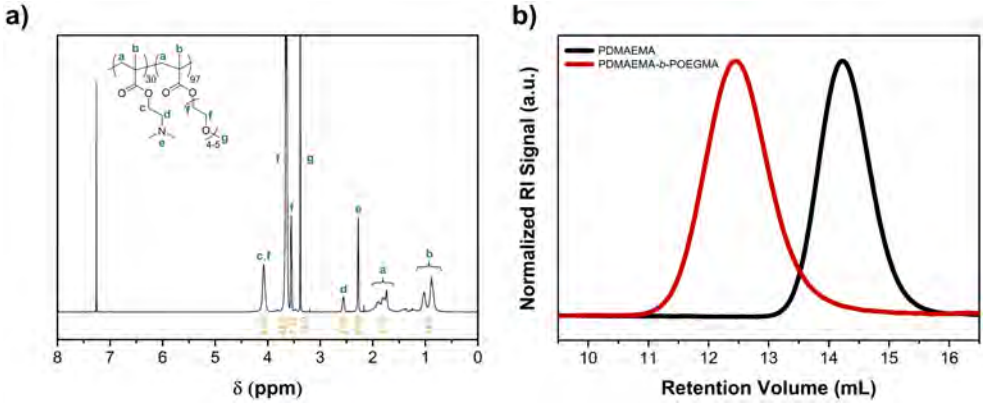

Figure 3.16. (a) ^{1}H NMR spectrum ($CDCl_3$) of the $PDMAEMA_{30}$-*b*-$POEGMA_{97}$ diblock copolymer. (b) GPC chromatograms (DMF) of the $PDMAEMA_{30}$ macro-CTA (black) and the $PDMAEMA_{30}$-*b*-$POEGMA_{97}$ diblock copolymer (red).

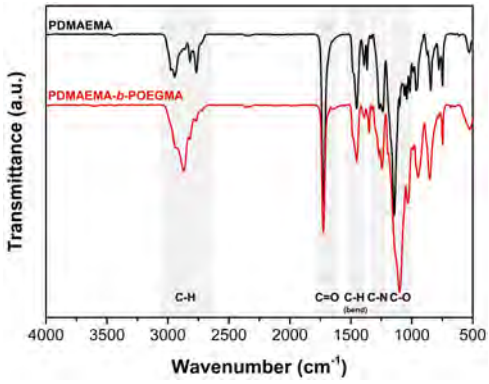

Figure 3.17. ATR-FTIR spectra of the synthesized PDMAEMA$_{30}$ macro-CTA (black) and the PDMAEMA$_{30}$-*b*-POEGMA$_{97}$ diblock copolymer (red).

3.4.9. Synthesis of PDMAEMA$_{30}$-*b*-PMPC$_{106}$

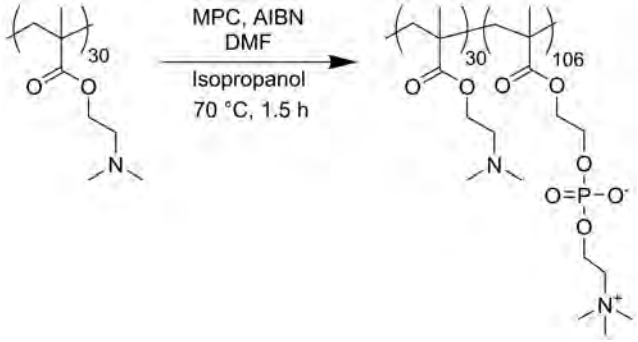

Scheme 3.13. Reaction scheme for the synthesis of the PDMAEMA$_{30}$-*b*-PMPC$_{106}$ diblock copolymer.

PDMAEMA$_{30}$ macro-CTA (1 eq., 0.0408 mmol, 200 mg), 2-methacryloyloxyethyl phosphorylcholine (MPC) monomer (151 eq., 6.17 mmol, 1.82 g), AIBN (0.1 eq., 0.0045 mmol, 0.738 mg – using 83.6 mg of an 8.3 mg mL^{-1} stock solution in DMF), DMF (300 eq., 1.34 mL), and isopropanol (900 eq., 4.22 mL) were charged in a 25 mL round-bottom flask equipped with a stirring bar and septum. The solvent mixture of DMF and isopropanol was required to ensure complete dissolution of both PDMAEMA and MPC. The reaction mixture was sparged with argon for 10 min. A t = 0 h ^{1}H NMR sample was taken towards the end of the degassing cycle. The flask was immersed in a thermostated oil bath at 70 °C. After 1.5 hours, the reaction mixture was quenched by cooling the flask in cold water and subsequently exposing it to air. A t = 1.5 h ^{1}H NMR sample was prepared in order to calculate the conversion through comparison of the DMF standard and MPC peaks (conv. = 61%). The reaction mixture was purified by precipitation into cold diethyl ether, after which it was redissolved in methanol and dialyzed against methanol/acetone over the course of several days to remove the

remainder of unreacted monomer. The polymer solution was concentrated *in vacuo* and dried at room temperature under high vacuum overnight. The yield of the yellow solid was determined (1.21 g, 98.2%) and the product was characterized by ^{1}H NMR (Figure 3.18a) and ATR-FTIR (Figure 3.18b).

^{1}H NMR (400 MHz, methanol-d_4): δ (ppm) = 4.30 (br, O-CH_2, PMPC), 4.19 (br, CH_2-O, PMPC), 4.05 (br, 2x O-CH_2, PDMAEMA and PMPC), 3.71 (br, CH_2-N, PMPC), 3.27 (br, N-$(CH_3)_3$, PMPC), 2.61 (br, CH_2-N, PDMAEMA), 2.30 (s, N-$(CH_3)_2$, PDMAEMA), 2.2–1.6 (br, CH_2, backbone), 1.2–0.5 (br, CH_3, backbone). Conversion = 61%, $M_{n,PMPC}$ = 31.3 kg mol^{-1}, $P_{n,PMPC}$ = 106. $M_{n,total}$ = 36.2 kg mol^{-1}. x_{PMPC} = 0.779, f_{PMPC} = 0.869.

The PDMAEMA-*b*-PMPC diblock copolymer was successfully synthesized in high purity, as evidenced by ^{1}H NMR (Figure 3.18a). The conversion of this zwitterionic polymer was deliberately kept low to avoid chain-chain coupling.[43] Comparison of the ATR-FTIR spectra also confirmed the successful addition of the PMPC block, evidenced by the emerging characteristic absorption bands of PMPC: the phosphate group (P=O stretch at 1233 cm^{-1} and P-O stretch at 1055 cm^{-1}) and the characteristic -$N^+(CH_3)_3$ stretching vibration at 954 cm^{-1} (Figure 3.18b). The broad band of the -OH stretch around 3300 cm^{-1} indicates the presence of water, which is in accordance with the hygroscopic nature of PMPC. Due to the unavailability of an aqueous GPC, and because of undesired interactions between the polymer and the GPC column when dissolved in DMF, characterization via GPC was not performed.

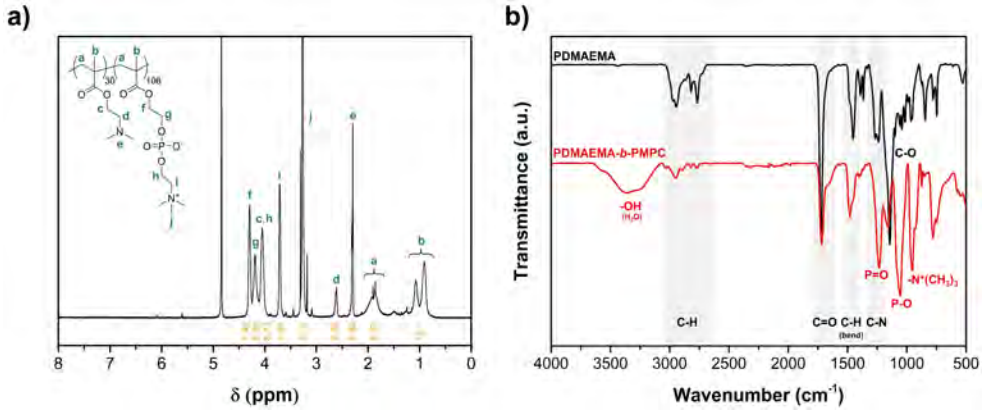

Figure 3.18. (a) ^{1}H NMR spectrum (methanol-d_4) of the $PDMAEMA_{30}$-*b*-$PMPC_{106}$ diblock copolymer. (b) ATR-FTIR spectra of the synthesized $PDMAEMA_{30}$ macro-CTA (black) and the $PDMAEMA_{30}$-*b*-$PMPC_{106}$ diblock copolymer (red).

3.5. ATRP – Synthesis and Analysis

3.5.1. Synthesis of the PEG_{90}-Br Macroinitiator

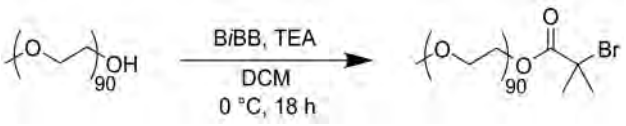

Scheme 3.14. Reaction scheme for the synthesis of the PEG_{90}-Br macroinitiator.

Poly(ethylene glycol) (PEG) homopolymer (M_n = 4.01 kg mol^{-1}, $Đ$ = 1.05) was purchased from TCI and was subsequently converted into a PEG-Br macroinitiator through esterification of the hydroxyl group by treatment with an excess of acid halide, a method adapted from an earlier reported procedure.[37]

PEG_{90}-OH (1 eq., 6.25 mmol, 25.1 g) was charged into a 250 mL three-neck round-bottom flask, equipped with a stirring bar and a tap connected to nitrogen. After several high-vacuum/nitrogen cycles to minimize residual moisture, 100 mL dry DCM and triethylamine (TEA) (1.5 eq., 9.38 mmol, 947 mg, 1304 µL) were added to the flask directly. The mixture was cooled using an ice bath, followed by the dropwise addition of α-bromoisobutyryl bromide (B*i*BB) (5 eq., 31.3 mmol, 718 mg, 386 µL) in 50 mL dry DCM, operated under a continuous flow of nitrogen. The reaction mixture was allowed to warm up to room temperature and was left to stir overnight. After about 18 hours, the unreacted B*i*BB was quenched by the addition of about 5 mL of ethanol. The solution was concentrated *in vacuo* and precipitated into cold *n*-hexane. The yellowish product was redissolved in DCM and the precipitation procedure was repeated once more. To completely remove all TEA, the polymer was recrystallized according to a previously reported procedure,[44] where the yellowish precipitate was redissolved in 200 mL warm ethanol (50 °C), cooled down in the fridge (4 °C), and centrifuged. The yellow supernatant was discarded and the recrystallization method was repeated several times (3–4x) until the supernatant remained completely colorless. The purified product was collected and dried in a vacuum oven (40 °C) overnight. The yield of the white powder was determined (22.5 g, 81.5%) and the product was characterized by ^{1}H NMR (Figure 3.19a), GPC (Figure 3.19b), and ATR-FTIR (Figure 3.21).

^{1}H NMR (400 MHz, $CDCl_3$): δ (ppm) = 4.31 (t, CH_2), 3.63 (br, O-CH_2), 3.36 (s, O-CH_3), 1.92 (s, 2x CH_3). M_n = 4.4 kg mol^{-1}, P_n = 90.

GPC (DMF): $M_{n,GPC}$ = 7.1 kg mol^{-1}, $Đ$ = 1.06.

The PEG_{90}-Br macroinitiator was successfully synthesized in high purity, as evidenced by the emerging peaks at 4.31 and 1.92 ppm seen in ^{1}H NMR (Figure 3.19a). As expected, the GPC spectra recorded before and after esterification are identical, which confirms a successful modification without side reactions (Figure 3.19b).

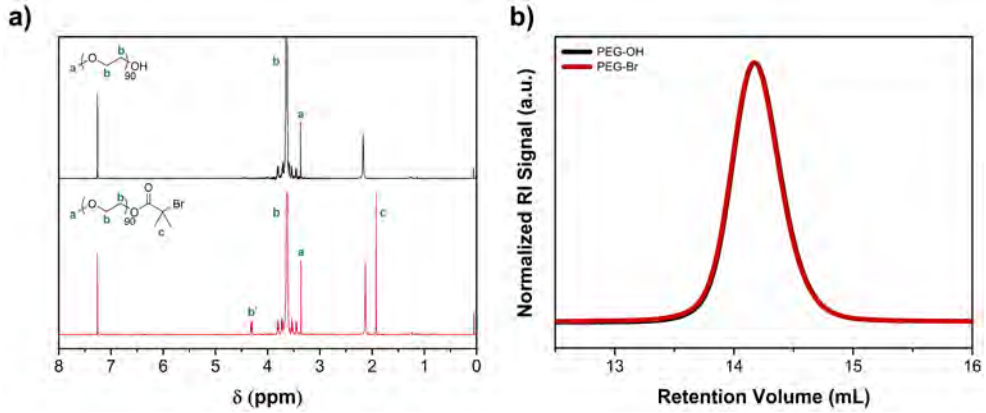

Figure 3.19. (a) ^{1}H NMR spectra ($CDCl_3$) and (b) GPC chromatograms (DMF) of PEG_{90}-OH (black) and the PEG_{90}-Br macroinitiator (red).

3.5.2. Synthesis of PEG_{90}-*b*-$PDMAEMA_x$ Diblock Copolymers

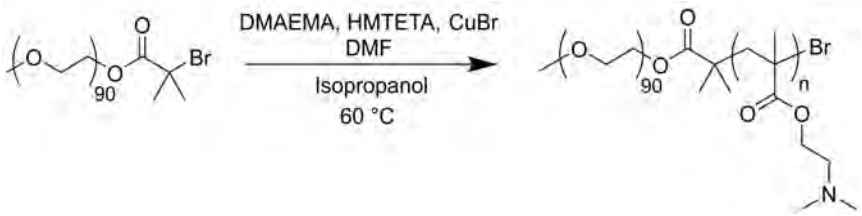

Scheme 3.15. Reaction scheme for the synthesis of PEG_{90}-*b*-$PDMAEMA_x$ diblock copolymers.

The reaction conditions for obtaining PEG_{90}-*b*-$PDMAEMA_x$ diblock copolymers with distinct block ratios and lengths are summarized in Table 3.6.

PEG_{90}-Br (1 eq.) and isopropanol (*i*-PrOH) were charged in a glass vial and carefully heated inside a warm water bath to ensure full dissolution of the PEG_{90}-Br macroinitiator. Purified DMAEMA, 1,1,4,7,10,10-hexamethyltriethylenetetramine (HMTETA) (1 eq.), and DMF (internal standard) were subsequently added to the mixture and everything was mixed until dissolved. The transparent reaction mixture was transferred to a Schlenk flask, equipped with a stirring bar and septum, and a t = 0 h ^{1}H NMR sample was taken. The reaction mixture was deoxygenated via three freeze-pump-thaw cycles, after which the reaction mixture was frozen once more and the copper(I) bromide (CuBr) catalyst powder (1 eq.) was carefully added on top of the frozen mixture with the argon/vacuum inlet closed. Afterwards, the flask was closed with a septum and the freeze-pump-thaw cycle was continued. During the final thaw step, the septum was punctured with a short needle to flush the flask with argon in order to remove any remaining oxygen. Once fully defrosted, the degassing cycle was stopped (removal of the outlet needle and closing of the inlet valve), and the flask was immersed in a thermostated oil bath at 60 °C to initiate the reaction. After 30 to 60

minutes, the green reaction mixture was quenched by cooling the flask in cold water and subsequently exposing it to air. A ^{1}H NMR sample was prepared in order to calculate the conversion through comparison of the DMF standard and DMAEMA peaks. The reaction mixture was precipitated once in *n*-hexane, redissolved in THF, and passed through a short aluminum oxide (basic) column to remove the excess of CuBr catalyst. The obtained polymer solution was dialyzed against methanol over the course of several days (≥3 days) to remove the remainder of the unreacted monomer and catalyst while frequently renewing the solvent. The polymer solution was concentrated *in vacuo* and further dried in a vacuum oven (40 °C) overnight. After drying, the yield of the white powder was determined and the product was characterized by ^{1}H NMR (Figure 3.20a), GPC (Figure 3.20b), and ATR-FTIR (Figure 3.21).

^{1}H NMR (400 MHz, $CDCl_3$): δ (ppm) = 4.05 (br, O-CH_2, PDMAEMA), 3.63 (s, 2x CH_2, PEG), 2.55 (br, CH_2-N, PDMAEMA), 2.27 (s, 2x N-CH_3, PDMAEMA), 2.05–1.70 (br, CH_2 backbone, PDMAEMA), 1.16–0.75 (br, CH_3 backbone, PDMAEMA).

The PEG_{90}-*b*-$PDMAEMA_x$ diblock copolymers were successfully synthesized in high purity, as evidenced by ^{1}H NMR (Figure 3.20a). GPC showed a clear shift to lower retention volumes indicative of a successful chain extension, albeit with somewhat higher dispersities than was initially recorded for the PEG_{90}-Br macroinitiator (Figure 3.20b). This can be explained by the slight shoulders seen, positioned exactly at the retention volume for PEG_{90}-Br, suggesting the presence of unreacted PEG_{90}-Br macroinitiator. Finally, comparison of the ATR-FTIR spectra also confirmed the successful addition of the PDMAEMA block, evidenced by the emerging characteristic C=O stretch (1724 cm^{-1}) and the broadened C-H stretching vibration (~3000 cm^{-1}) (Figure 3.21).

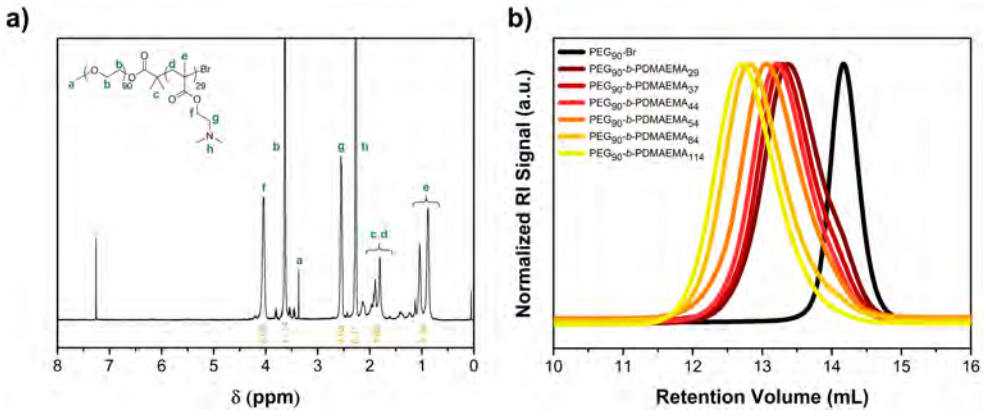

Figure 3.20. (a) ^{1}H NMR spectrum ($CDCl_3$) of a typical PEG-*b*-PDMAEMA diblock copolymer (PEG_{90}-*b*-$PDMAEMA_{29}$). (b) GPC chromatograms (DMF) of the PEG_{90}-Br macroinitiator (black) and all PEG_{90}-*b*-$PDMAEMA_x$ diblock copolymers (red-yellow).

Table 3.6. Reaction conditions for the synthesis of PEG_{90}-*b*-$PDMAEMA_x$ diblock copolymers by ATRP. The subscripts denote the degree of polymerization of each block. Amounts of reactants are given in mmol and solvents in mL. Reaction times (t_R) are in minutes, conversions were determined by ^1H NMR (%), yields are given in %, and molecular weights (M_n) are reported in kg mol^{-1}. $f_{PDMAEMA}$ represents the weight fraction of PDMAEMA and $M_{n,calc}$ is the sum of the calculated molecular weights based on the initial concentrations and monomer conversion ($M_{n,PEG}$ + $M_{n,PDMAEMA}$). $M_{n,GPC}$ and the molecular weight distribution ($Đ$) were determined by GPC.

Polymer	PEG_{90}-Br	DMAEMA	HMTETA	CuBr	DMF	*i*-PrOH	t_R	Conv.	Yield	$f_{PDMAEMA}$	$M_{n,calc}$	$M_{n,GPC}$	$Đ$
PEG_{90}-*b*-$PDMAEMA_{29}$	0.24 (1 eq.)	12.1 (50 eq.)	0.24 (1 eq.)	0.24 (1 eq.)	0.94	7.8	30	59.1	82.2	0.53	8.7	13.8	1.22
PEG_{90}-*b*-$PDMAEMA_{37}$	0.12 (1 eq.)	8.45 (70 eq.)	0.12 (1 eq.)	0.12 (1 eq.)	0.65	3.9	30	53.8	87.0	0.59	10.0	14.2	1.21
PEG_{90}-*b*-$PDMAEMA_{44}$	0.12 (1 eq.)	8.45 (70 eq.)	0.12 (1 eq.)	0.12 (1 eq.)	0.65	3.9	45	63.4	93.7	0.63	11.1	15.4	1.20
PEG_{90}-*b*-$PDMAEMA_{54}$	0.12 (1 eq.)	8.45 (70 eq.)	0.12 (1 eq.)	0.12 (1 eq.)	0.65	2.0	60	75.3	60.2	0.68	12.5	17.2	1.25
PEG_{90}-*b*-$PDMAEMA_{84}$	0.12 (1 eq.)	24.2 (200 eq.)	0.12 (1 eq.)	0.12 (1 eq.)	1.9	14.8	60	42.0	ND	0.77	17.3	20.6	1.27
PEG_{90}-*b*-$PDMAEMA_{114}$	0.12 (1 eq.)	24.2 (200 eq.)	0.12 (1 eq.)	0.12 (1 eq.)	1.9	22.2	60	38.3	ND	0.82	22.1	23.6	1.25

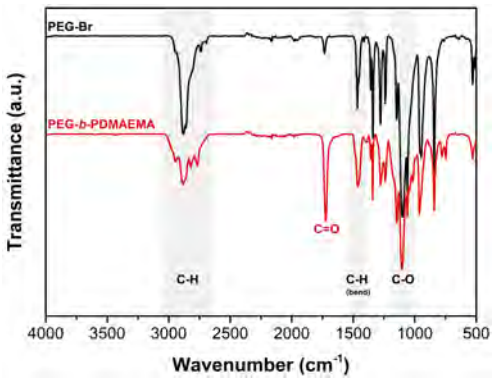

Figure 3.21. ATR-FTIR spectra of the PEG_{90}-Br macroinitiator (black) and the PEG_{90}-*b*-$PDMAEMA_{29}$ diblock copolymer (red).

3.5.3. Quaternization of PEG_{90}-*b*-$PDMAEMA_{29}$

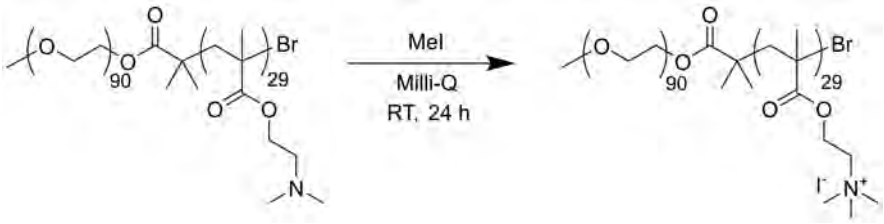

Scheme 3.16. Reaction scheme for the quaternization of the PEG_{90}-*b*-$PDMAEMA_{29}$ diblock copolymer.

The weak polyelectrolyte PEG_{90}-*b*-$PDMAEMA_{29}$ (1 eq., 200 mg, 0.666 mmol DMAEMA, 105 mg DMAEMA) was charged into a 20 mL glass vial, equipped with a stirring bar. A volume of 10 mL Milli-Q water was introduced to disperse the polymer before the addition of iodomethane (MeI) reagent (5 eq., 2.95 mmol, 418 mg). The reaction was left to stir at room temperature for 24 hours, after which it was sparged with nitrogen for 4 hours to evaporate the excess of reagent. The obtained strong polyelectrolyte was freeze-dried to yield a white powder (277 mg, 97.8%), which was characterized by ^{1}H NMR (Figure 3.22a).

^{1}H NMR (400 MHz, D_2O): δ (ppm) = 4.55 (br, O-CH2, PMETAI), 3.90 (br, CH_2-N, PMETAI), 3.69 (s, 2x CH_2, PEG), 3.33 (br, 3x N-CH_3, PMETAI), 2.08 (br, CH_2 backbone, PMETAI), 1.3–0.85 (br, CH_3 backbone, PMETAI). Degree of quaternization ≥ 95%. $M_{n,PEG\text{-}Br}$ = 4.14 kg mol^{-1}, $M_{n,PMETAI}$ = 8.68 kg mol^{-1}, $M_{n,total}$ =12.8 kg mol^{-1}.

Quaternization of the DMAEMA units into 2-(methacryloyloxy)ethyl trimethyl ammonium iodide (METAI) units was confirmed by ^{1}H NMR: the integration ratio between the side chain CH_2 and CH_3 signals increased from 2:6 to 2:9, indicating the presence of three methyl groups instead of two (Figure 3.22a). In addition, the strong

shift of these CH_2 and CH_3 peaks further confirmed a successful methylation (Figure 3.22b). Due to the unavailability of an aqueous GPC, and because of undesired interactions between the polymer and the GPC column when dissolved in DMF, characterization via GPC was not performed.

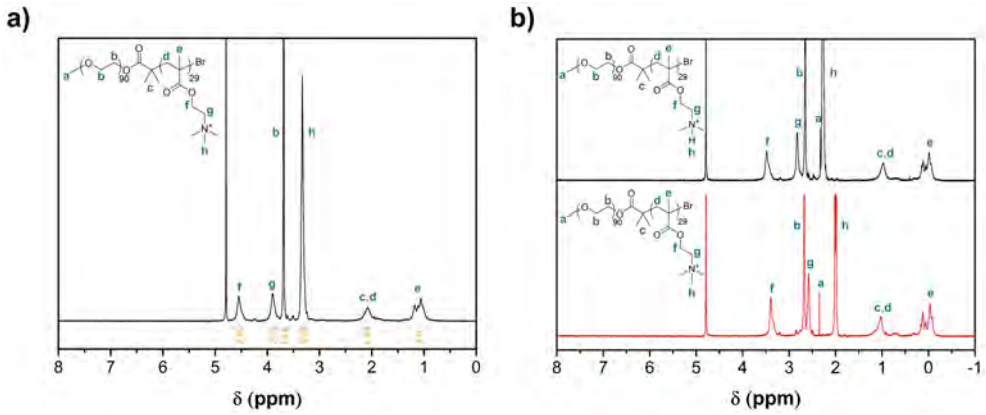

Figure 3.22. (a) ^{1}H NMR spectrum (D_2O) of the PEG_{90}-*b*-$PMETAI_{29}$ diblock copolymer. (b) ^{1}H NMR spectra ($DCl:D_2O$ – 1:5) of PEG_{90}-*b*-$PDMAEMA_{29}$ (black) and PEG_{90}-*b*-$PMETAI_{29}$ (red). The overall strong downfield shift observed for both spectra is related to the lowered pH.

3.6. Chain Transfer Agent (CTA) Removal

RAFT-synthesized polymers are functionalized by end-groups originating from the RAFT agent. In many applications, this does not pose an issue, since it only presents a minor fraction of the entire polymer chain. However, for low molecular weight polymers, which concerns several of the synthesized polymers presented in this thesis, the incorporation of sufficiently large and hydrophobic end-groups could cause undesirable effects, which may affect the final polymer properties. To illustrate this, in the case of an AB diblock copolymer like PS_{32}-*b*-PAA_{100}, the incorporated hydrophobic dodecyl chain of the DDMAT RAFT agent may give it an ABA triblock copolymer-like character. This could affect its properties in solution (e.g., solubility, critical aggregation concentration, and/or micellar shape), which can consequently hinder the formation of an effective antifouling coating.[34]

Hence, to investigate whether the incorporated end-groups of DDMAT affect the solubility and adsorption behavior of PS-*b*-PAA, and possibly the antifouling efficacy of the formed coating, it was decided to execute a complete CTA end-group removal according to a previously reported metal-free photocatalytic strategy.[36]

3.6.1. CTA Removal: PS_{27} Macro-CTA

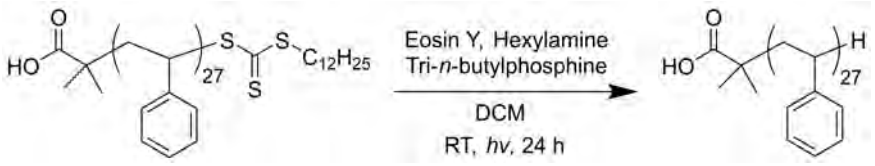

Scheme 3.17. Reaction scheme for the CTA end-group removal from the PS_{27} macro-CTA.

While under nitrogen atmosphere, PS_{27} macro-CTA (1 eq., 0.019 mmol, 60 mg) and 1 mL of DCM were charged in a 25 mL two-neck round-bottom flask, equipped with a stirring bar and septum, and a tap connected to nitrogen. After complete dissolution, the photocatalyst Eosin Y (0.05 eq., 0.944 μmol, 0.653 mg), hexylamine (12 eq., 0.227 mmol, 22.9 mg, 29.8 μL), and tri-*n*-butylphosphine (3 eq., 0.057 mmol, 11.5 mg, 14.0 μL) were added to the flask under nitrogen atmosphere via stock solutions in DCM. The reaction mixture was sparged with nitrogen for 10 min, after which it was irradiated with blue LED light for 24 hours to activate the photocatalyst. The polymer mixture was diluted with a small amount of methanol and added dropwise to a 50 mL centrifuge tube containing thoroughly stirred deionized water. The precipitated polymer was centrifuged at 4500 rpm for 5 min to facilitate complete precipitation. The polymer product was collected, redissolved in DCM, and the precipitation procedure was repeated. The purified polymer was collected and dried in a vacuum oven (40 °C) overnight to yield a white powder. The careful removal of the trithiocarbonate moiety was confirmed by UV-Vis (Figure 3.23a), GPC (Figure 3.23b), and ^{1}H NMR (Figure 3.24).

^{1}H NMR (400 MHz, $CDCl_3$): δ (ppm) = 7.30–6.30 (br, 5 CH, aromatic ring), 2.30–1.70 (br, CH), 1.70–1.30 (br, CH_2).

It is well known that end-capped RAFT agents can cause discoloration of the final product, which appears to be yellow in the case of trithiocarbonates like DDMAT.[22] Regarding CTA removal protocols, this discoloration presents an advantage: a loss of color will confirm the successful removal of the trithiocarbonate end-group. Indeed, after the photocatalytic protocol, the obtained polymer appears white rather than yellow (Figure 3.23a). The successful modification to PS-H was also supported by UV-Vis analysis: the strong absorbance of the trithiocarbonate moiety of PS-CTA around 315 nm (blue light, seen by humans as yellow) has completely disappeared (Figure 3.23a). Moreover, the GPC chromatogram of the PS-H product showed a single peak with low dispersity, nearly identical to that of PS-CTA (Figure 3.23b). The lack of shoulder(s) at low retention volumes implies the absence of undesirable disulfide coupling, which eliminates the possibility of having synthesized PS-SH instead of PS-H.[36,45]

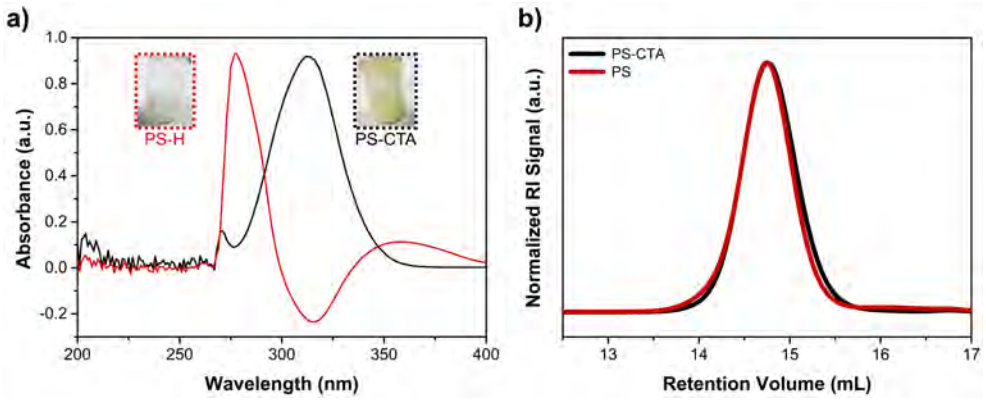

Figure 3.23. (a) UV-Vis spectra (THF) and (b) GPC chromatograms (DMF) of the PS_{27} macro-CTA before (black) and after (red) the photocatalytic protocol.

Finally, thorough analysis of the ^{1}H NMR data also confirmed a successful removal of the CTA: the characteristic CTA triplet peak assigned to the methylene proton next to the trithiocarbonate at 3.26 ppm disappeared (Figure 3.24, circle). If a thiol group would remain (PS-SH instead of PS-H), the peak corresponding to the methine proton (HS-CH(Ph)-) positioned at 5.03–4.60 ppm would shift to 3.65–3.40 ppm, but this shift was not observed (Figure 3.24, square).[45] Hence, the PS-CTA has been successfully converted to PS-H.

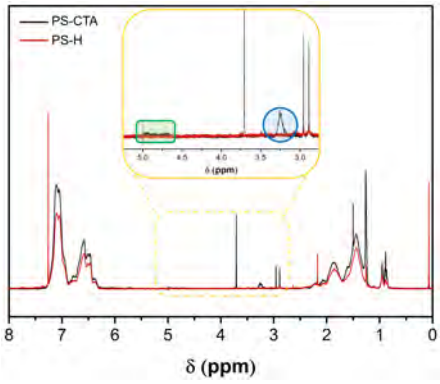

Figure 3.24. ^{1}H NMR spectra ($CDCl_3$) of the PS_{27} macro-CTA before (black) and after (red) the photocatalytic protocol.

3.6.2. CTA Removal: PS_{27}-*b*-P*t*BA_{338} Diblock Copolymer

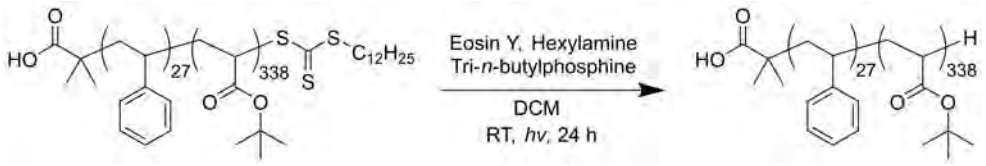

Scheme 3.18. Reaction scheme for the CTA end-group removal from the PS_{27}-*b*-P*t*BA_{338} diblock copolymer.

While under nitrogen atmosphere, PS_{27}-*b*-P*t*BA_{338} (1 eq., 0.011 mmol, 500 mg) and 1 mL of DCM were charged in a 25 mL two-neck round-bottom flask, equipped with a stirring bar and septum, and a tap connected to nitrogen. After complete dissolution, the photocatalyst Eosin Y (0.05 eq., 0.538 µmol, 0.372 mg), hexylamine (12 eq., 0.129 mmol, 13.1 mg, 17.0 µL), and tri-*n*-butylphosphine (3 eq., 0.032 mmol, 6.53 mg, 7.96 µL) were added to the flask under nitrogen atmosphere via stock solutions in DCM. The reaction mixture was sparged with nitrogen for 10 min, after which it was irradiated with blue LED light for 24 hours to activate the photocatalyst. The polymer mixture was diluted with a small amount of methanol and added dropwise to a 50 mL centrifuge tube containing thoroughly stirred deionized water. The precipitated polymer was centrifuged at 4500 rpm for 5 min to facilitate complete precipitation. The polymer product was collected, redissolved in DCM, and the precipitation procedure was repeated. The purified polymer was collected and dried in a vacuum oven (40 °C) overnight. The yield of the white powder was determined (0.33 g, 66.6%) and the removal of the trithiocarbonate moiety was confirmed by UV-Vis (Figure 3.25a) and GPC (Figure 3.25b). For successive self-assembly and antifouling experiments, the polymer was deprotected to give PS-*b*-PAA according to the previously discussed HFIP/HCl method (Section 3.4.3) and was subsequently characterized by ^{1}H NMR (Figure 3.26) and DLS (Figure 3.27).

The successful CTA removal was confirmed by comparison of the recorded UV-Vis spectra: the strong absorbance of the trithiocarbonate moiety around 315 nm completely disappeared after having followed the photocatalytic protocol (Figure 3.25a). Comparison of the GPC chromatograms before and after the photocatalytic protocol (Figure 3.25b) again confirms a successful removal of the CTA: shoulder(s) indicative of disulfide coupling are absent, so modification did not lead to PS-SH. Due to the high molecular weight of the PAA block, a loss of the characteristic CTA signals around 3.26 and 5.03–4.60 ppm is no longer clearly visible in ^{1}H NMR (Figure 3.26).

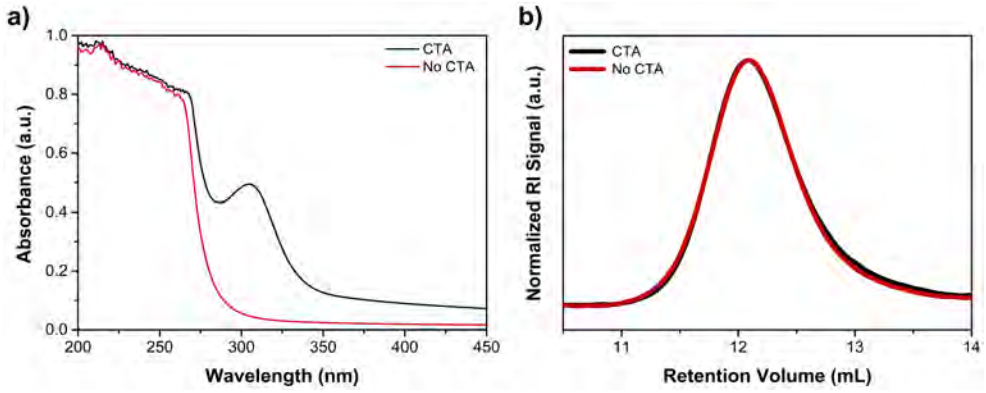

Figure 3.25. (a) UV-Vis spectra (THF) and (b) GPC chromatograms (DMF) of the PS_{27}-*b*-P*t*BA_{338} diblock copolymer before (black) and after (red) the photocatalytic protocol.

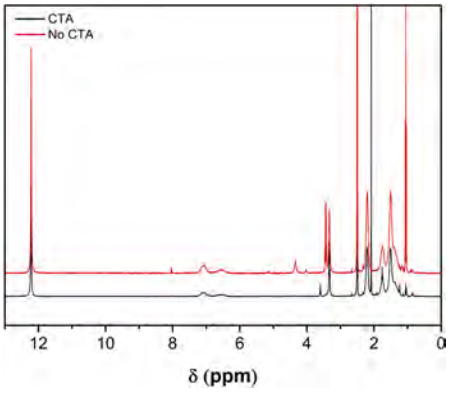

Figure 3.26. ^{1}H NMR spectra (DMSO-d_6) of the PS_{27}-*b*-PAA_{338} diblock copolymer with (black) and without (red) end-capped RAFT agent.

While Chong et al.[36] discovered an increase of particle size after the reduction of their polymer, related to a micellar shape change from flower-like to spherical, CTA removal did not change our polymer properties in solution at all, as evidenced by DLS: with or without end-capped CTA, both PS_{27}-*b*-PAA_{338} polymers dissolved as individual moieties, which could aggregate into larger structures (Figure 3.27). However, the diblock copolymers used in the work of Chong et al. were much smaller in length (n = 10, m = 34) and had a higher PS content (PS/PAA block ratio = 0.3). Clearly, the long PAA block of PS_{27}-*b*-PAA_{338} (block ratio = 0.08) forced the relatively small PS block into solution and hindered the formation of micelles, independent of having a C12 chain attached. Instead, to accurately determine the effect of the CTA on micellization, a polymer with a more comparable block ratio should be investigated, such as PS_{32}-*b*-PAA_{100}. Nevertheless, based on the current results, it is expected that the presence of CTA end-groups should not affect the development and performance of the resulting antifouling coating, which is further discussed in Chapter 5.

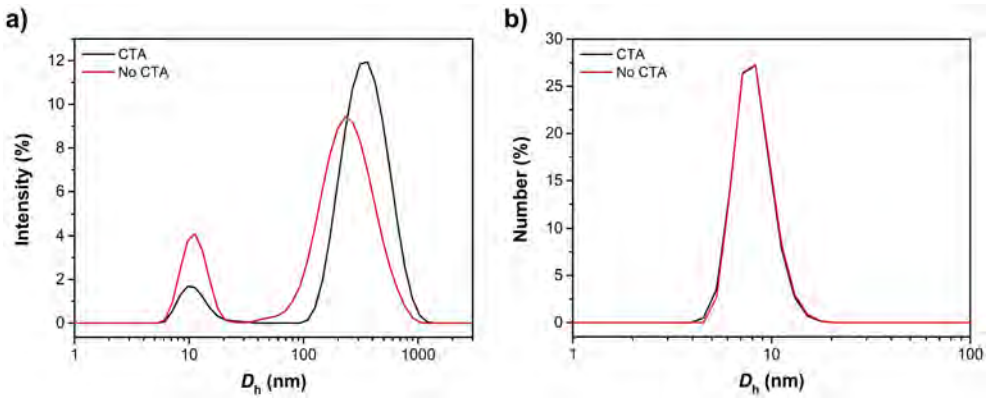

Figure 3.27. Size distribution plots of PS_{27}-*b*-PAA_{338} in ethanol with (black) and without (red) end-capped RAFT agent, including the (a) intensity plot and (b) number plot.

3.7. Conclusions

This chapter reported the successful synthesis of a library of polymers with various lengths and compositions for antifouling purposes, including PS, PMMA, PAA, PS-*b*-PAA, PMMA-*b*-PAA, PDMAEMA-*b*-PEG, PDMAEMA-*b*-POEGMA, and PDMAEMA-*b*-PMPC. All macro-CTAs, homopolymers, and diblock copolymers were successfully synthesized in high purity and with low dispersities, evidenced by a combination of ^{1}H NMR, GPC, and ATR-FTIR. The diblock copolymers always exhibited somewhat higher dispersities than their homopolymer counterparts, indicated by a slight peak tailing or the presence of a minor shoulder, suggesting slow initiation, premature termination, the occurrence of chain-chain coupling, and/or the presence of unreacted homopolymer. By straightforward methylation of PDMAEMA, the PEG-*b*-PDMAEMA diblock copolymer was successfully converted into a quaternized and strong polyelectrolyte (PEG-*b*-PMETAI). Finally, it was shown that the incorporated DDMAT RAFT agent could be successfully removed from both PS and PS-*b*-P*t*BA via a photocatalytic strategy with Eosin Y: the characteristic trithiocarbonate signals in ^{1}H NMR and UV-Vis disappeared, while GPC indicated no signs of disulfide coupling. Moreover, the successful photocatalytic CTA removal did not affect the polymer properties in solution: with or without end-capped CTA, both PS-*b*-PAA polymers dissolved as individual moieties, which could aggregate into larger structures.

References

[1] C. M. Magin, S. P. Cooper, A. B. Brennan, *Mater. Today* **2010**, *13*, 36.
[2] A. Alghunaim, B. M. Zhang Newby, *Colloids Surf B Biointerfaces* **2016**, *140*, 514.
[3] A. M. C. Maan, A. H. Hofman, W. M. de Vos, M. Kamperman, *Adv. Funct. Mater.* **2020**, *30*, 2000936.
[4] B. Kronberg, K. Holmberg, B. Lindman, *Surface Chemistry of Surfactants and Polymers, First Edition. Definition of a Surfactant*; 2014.
[5] E. Spruijt, *PhD Thesis: Strength, structure and stability of polyelectrolyte complex coacervates*; 2012.
[6] A. Halperin, D. E. Leckband, *Comptes Rendus l'Academie des Sci. - Ser. IV Physics, Astrophys.* **2000**, *1*, 1171.
[7] S. T. Milner, *Science* **1991**, *251*, 905.
[8] E. P. K. Currie, W. Norde, M. A. Cohen Stuart, *Adv. Colloid Interface Sci.* **2003**, *100–102*, 205.
[9] W. M. de Vos, T. Cosgrove, J. M. Kleijn, A. de Keizer, M. A. Cohen Stuart, Polymer Brushes. *Kirk-Othmer Encycl. Chem. Technol. Wiley Sons Inc.* **2010**, 1–22.
[10] W. M. de Vos, G. Meijer, A. de Keizer, M. A. Cohen Stuart, J. M. Kleijn, *Soft Matter* **2010**, *6*, 2499.
[11] Y. J. Oh, E. S. Khan, A. del Campo, P. Hinterdorfer, B. Li, *ACS Appl. Mater. Interfaces* **2019**, *11*, 29312.
[12] Z. Cao, T. Gan, G. Xu, C. Ma, *Langmuir* **2019**, *35*, 14596.
[13] B. Hofs, A. Brzozowska, A. de Keizer, W. Norde, M. A. Cohen Stuart, *J. Colloid Interface Sci.* **2008**, *325*, 309.
[14] S. Chen, L. Li, C. Zhao, J. Zheng, *Polymer* **2010**, *51*, 5283.
[15] A. M. Brzozowska, B. Hofs, A. de Keizer, R. Fokkink, M. A. Cohen Stuart, W. Norde, *Colloids Surfaces A Physicochem. Eng. Asp.* **2009**, *347*, 146.
[16] W. M. de Vos, J. M. Kleijn, M. A. Cohen Stuart, In *Polymer Brushes: Substrates, Technologies, and Properties*; 2012; pp. 133–162.
[17] L. I. Klushin, A. M. Skvortsov, A. A. Polotsky, A. S. Ivanova, F. Schmid, *J. Chem. Phys.* **2021**, *154*, 074904
[18] G. J. Fleer, M. A. Cohen Stuart, J. M. H. M. Scheutjens, T. Cosgrove, B. Vincent, *Polymers At Interfaces*; Chapman & Hall, London, 1993.
[19] J. J. Keating, J. Imbrogno, G. Belfort, *ACS Appl. Mater. Interfaces* **2016**, *8*, 28383.
[20] C. Marques, J. F. Joanny, L. Leibler, *Macromolecules* **1988**, *21*, 1051.
[21] C. M. Marques, J. F. Joanny, *Macromolecules* **1989**, *22*, 1454.
[22] S. Perrier, *Macromolecules* **2017**, *50*, 7433.
[23] J. Chiefari, Y. K. Chong, F. Ercole, J. Krstina, J. Jeffery, T. P. T. Le, R. T. A. Mayadunne, G. F. Meijs, C. L. Moad, G. Moad, E. Rizzardo, S. H. Thang, *Macromolecules* **1998**, *31*, 5559.
[24] C. Boyer, V. Bulmus, T. P. Davis, V. Ladmiral, J. Liu, S. Perrier, *Chem. Rev.* **2009**, *109*, 5402.
[25] S. Perrier, P. Takolpuckdee, *J. Polym. Sci. Part A Polym. Chem.* **2005**, *43*, 5347.
[26] N. P. Truong, G. R. Jones, K. G. E. Bradford, D. Konkolewicz, A. Anastasaki, *Nat. Rev. Chem.* **2021**, *5*, 859.
[27] G. Moad, E. Rizzardo, S. H. Thang, *Polymer* **2008**, *49*, 1079.
[28] K. Matyjaszewski, N. V. Tsarevsky, *J. Am. Chem. Soc.* **2014**, *136*, 6513.
[29] J. Ran, L. Wu, Z. Zhang, T. Xu, *Prog. Polym. Sci.* **2014**, *39*, 124.
[30] D. J. Siegwart, J. K. Oh, K. Matyjaszewski, *Prog. Polym. Sci.* **2012**, *37*, 18.
[31] D. J. Keddie, *Chem. Soc. Rev.* **2014**, *43*, 496.
[32] K. Matyjaszewski, *Isr. J. Chem.* **2012**, *52*, 206.
[33] K. Matyjaszewski, *Adv. Mater.* **2018**, *30*, 1.
[34] J. Y. T. Chong, D. J. Keddie, A. Postma, X. Mulet, B. J. Boyd, C. J. Drummond, *Colloids Surfaces A Physicochem. Eng. Asp.* **2015**, *470*, 60.
[35] J. Du, H. Willcock, J. P. Patterson, I. Portman, R. K. O'Reilly, *Small* **2011**, *7*, 2070.
[36] E. H. Discekici, S. L. Shankel, A. Anastasaki, B. Oschmann, I. H. Lee, J. Niu, A. J. McGrath, P. G. Clark, D. S. Laitar, J. R. de Alaniz, C. J. Hawker, D. J. Lunn, *Chem. Commun.* **2017**, *53*, 1888.
[37] T. Pelras, A. H. Hofman, L. M. H. Germain, A. M. C. Maan, K. Loos, M. Kamperman, *Macromolecules* **2022**, *55*, 8795.
[38] A. H. Hofman, R. Fokkink, M. Kamperman, *Polym. Chem.* **2019**, *10*, 6109.

[39] M. Obata, S. Tanaka, H. Mizukoshi, E. Ishihara, M. Takahashi, S. Hirohara, *J. Polym. Sci. Part A Polym. Chem.* **2018**, *56*, 560.
[40] A. D. Filippov, I. A. van Hees, R. Fokkink, I. K. Voets, M. Kamperman, *Macromolecules* **2018**, *51*, 8316.
[41] T. Wu, P. Gong, I. Szleifer, P. Vlček, V. Šubr, J. Genzer, *Macromolecules* **2007**, *40*, 8756.
[42] K. A. Davis, K. Matyjaszewski, *Macromolecules* **2000**, *33*, 4039.
[43] T. Pelras, Nonappa, C. S. Mahon, M. Müllner, *Macromol. Rapid Commun.* **2020**, *42*, 2000401.
[44] T. I. Löbling, J. S. Haataja, C. V. Synatschke, F. H. Schacher, M. Müller, A. Hanisch, A. H. Gröschel, A. H. E. Müller, *ACS Nano* **2014**, *8*, 11330.
[45] S. S. Zhang, K. Cui, J. Huang, Q. L. Zhao, S. K. Cao, Z. Ma, *RSC Adv.* **2015**, *5*, 44571.

Appendix A – Additional Theory, GPC, and Polymer Library

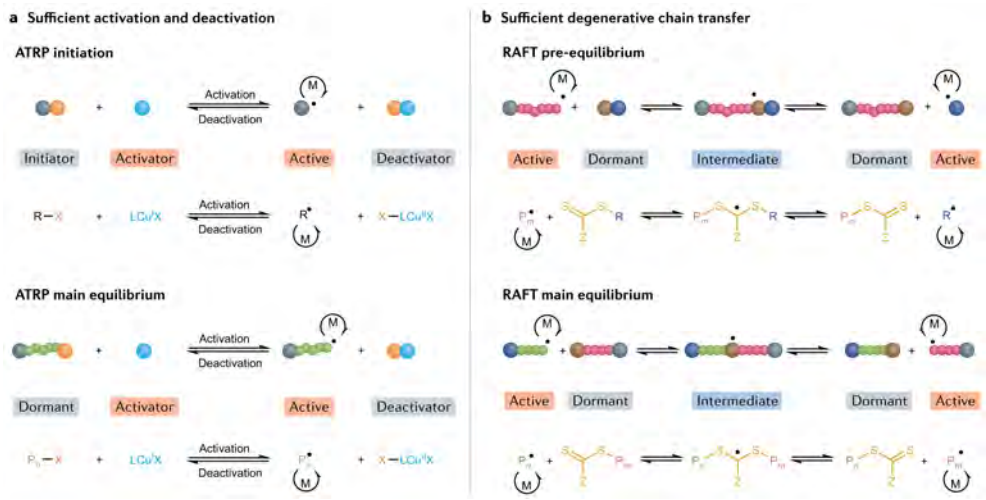

Figure A1. Illustrated mechanisms of (a) ATRP and (b) RAFT, including their main equilibrium state. Reproduced with permission.[26] Copyright 2021, Springer Nature.

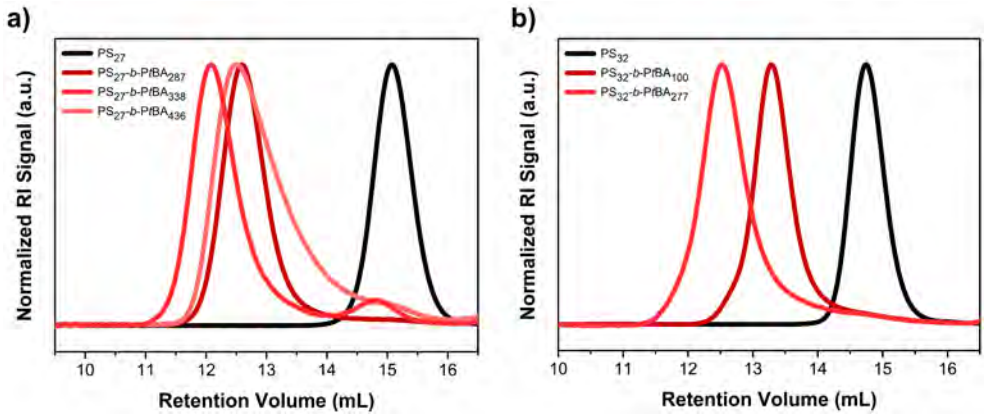

Figure A2. GPC chromatograms (DMF) of (a) the PS_{27} macro-CTA (black) and the PS_{27}-*b*-P*t*BA$_x$ diblock copolymers (red), and (b) the PS_{32} macro-CTA (black) and the PS_{32}-*b*-P*t*BA$_x$ diblock copolymers (red).

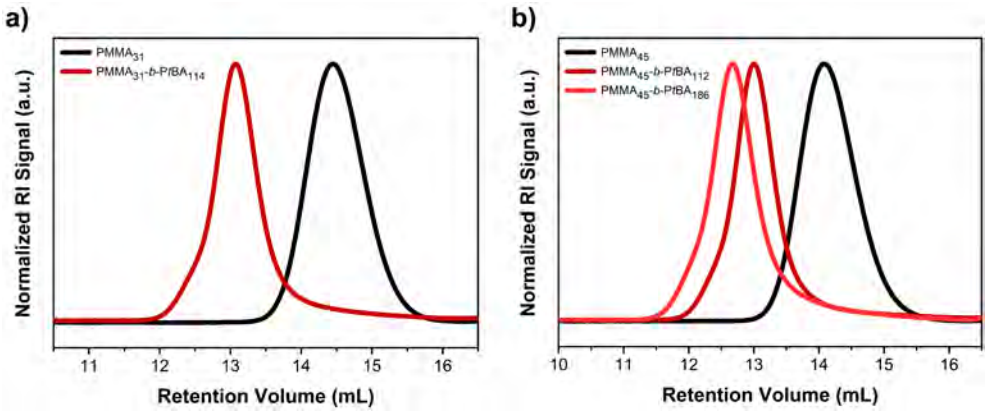

Figure A3. GPC chromatograms (DMF) of (a) the $PMMA_{31}$ macro-CTA (black) and the $PMMA_{31}$-*b*-P*t*BA_{114} diblock copolymer (red), and (b) the $PMMA_{45}$ macro-CTA (black) and the $PMMA_{45}$-*b*-P*t*BA_x diblock copolymers (red).

Table A1. Overview of all synthesized homopolymers and diblock copolymers, where M_n corresponds to the calculated molecular weight (kg mol^{-1}) determined by ^1H NMR, *n* and *m* are the degrees of polymerization, and *Đ* represents the molecular weight distribution.

Polymer	***n*** (block 1)	***m*** (block 2)	M_n	***Đ***
PS	27	-	3.2	1.14
	32	-	3.7	1.10
	47	-	5.3	1.08
	55	-	6.1	1.07
	81	-	8.8	1.09
	85	-	9.2	1.09
	87	-	9.4	1.09
	90	-	9.7	1.09
PS-*b*-P*t*BA	32	100	16.5	1.27
	32	277	39.1	1.53
	27	287	40.0	1.20
	27	338	46.5	1.30
	27	436	59.1	1.79
	81	79	18.9	1.17
	81	81	19.2	1.15
	85	81	19.6	1.15
PS-*b*-PAA	32	100	10.9	-
	32	277	23.6	-
	27	287	23.9	-
	27	338	27.5	-
	27	436	34.6	-
	81	79	14.5	-
				-

	81	81	14.6	-
	85	81	15.0	
PMMA	31	-	3.3	1.18
	45	-	4.8	1.20
	80	-	8.2	1.24
	90	-	9.2	1.26
	207	-	21.0	1.25
	486	-	48.0	1.40
PMMA-*b*-P*t*BA	31	114	17.9	1.47
	45	112	19.1	1.41
	80	186	28.9	1.44
	90	118	23.2	1.40
	207	113	23.6	1.46
	486	184	32.8	1.42
PMMA-*b*-PAA	31	114	11.5	-
	45	112	12.8	-
	80	186	18.3	-
	90	118	16.6	-
	207	113	17.3	-
	486	184	22.5	-
P*t*BA	107	-	13.7	1.14
	120	-	15.4	1.13
	142	-	18.2	1.14
PAA	107	-	7.7	-
	120	-	8.7	-
	142	-	10.2	-
PDMAEMA	30	-	4.9	1.17
PDMAEMA-*b*-POEGMA	30	97	34.0	1.28
PDMAEMA-*b*-PMPC	30	106	36.2	-
PEG-Br	90	-	4.4	1.06
PEG-*b*-PDMAEMA	90	29	8.7	1.22
	90	37	10.0	1.21
	90	44	11.1	1.20
	90	54	12.5	1.25
	90	84	17.3	1.27
	90	114	22.1	1.25
PEG-*b*-PMETAI	90	29	12.8	-